



University Mohamed Khider of Biskra  
Faculty of Exact Sciences and Science of Nature and Life  
Department of Matter Sciences

## Master Thesis

Domain of matter physics  
Section of Physics  
Condensed matter physics

Réf. : Entrez la référence du document

---

Presented by:  
**Gherbia Linda**  
**Gherbia Siham**

Le : 25-9-2020

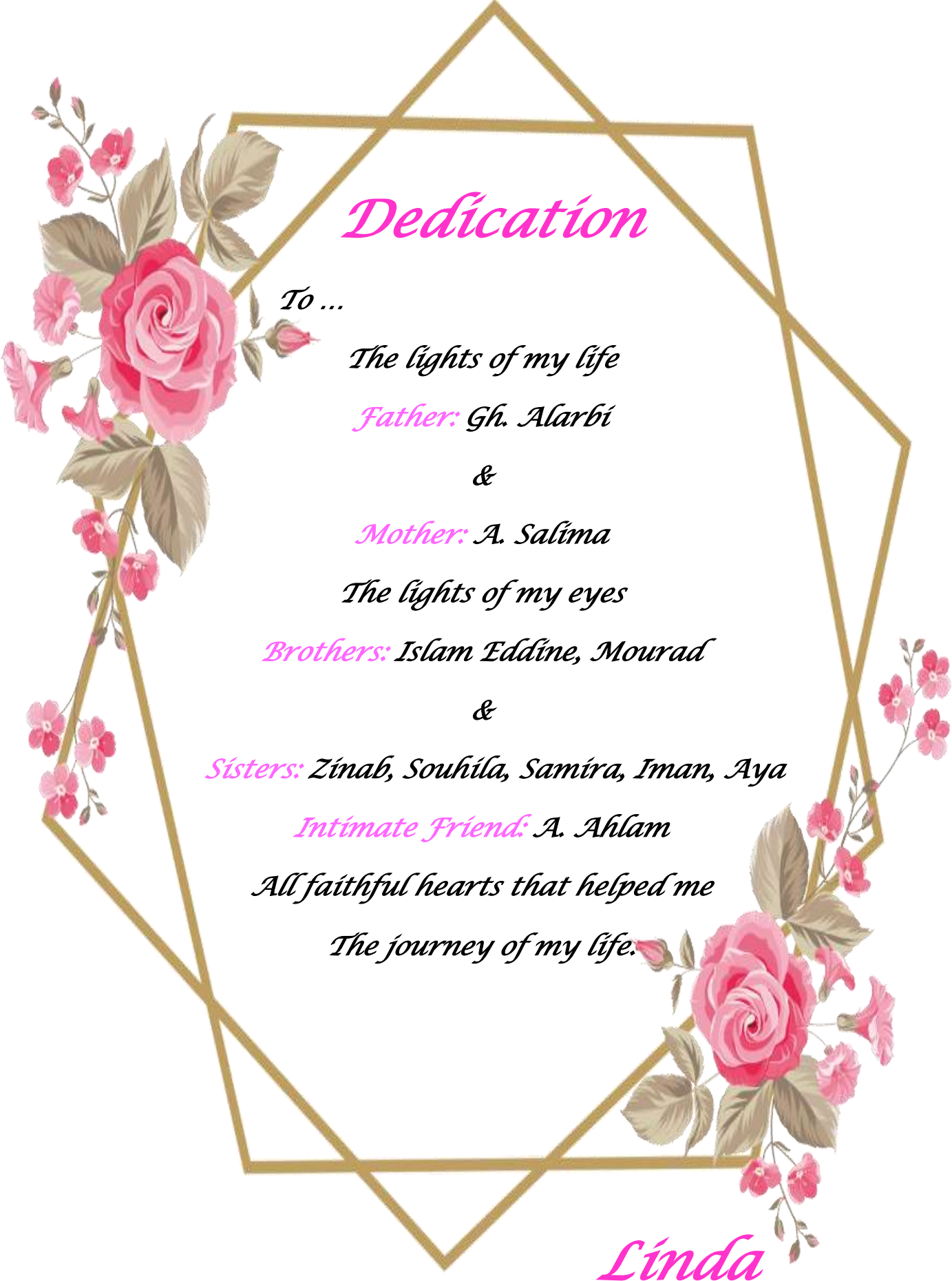
# Synthesis and Characterization of Mg Doped CuO Thin films.

---

### The Jury:

Lakel Said	Professor	University Med Khider - Biskra	President
Almi kenza	M.C.«B»	University Med Khider - Biskra	Supervisor
Boudour Bariza	M.C.«B»	University Med Khider - Biskra	Examiner





# *Dedication*

*To ...*

*The lights of my life*

*Father: Gh. Alarbi*

*&*

*Mother: A. Salima*

*The lights of my eyes*

*Brothers: Islam Eddine, Mourad*

*&*

*Sisters: Zinab, Souhila, Samira, Iman, Aya*

*Intimate Friend: A. Ahlam*

*All faithful hearts that helped me*

*The journey of my life.*

*Linda*



## *Dedication*

*To ....*

*The spring of tenderness and safety*

*My mother & father.*

*All my dear brothers & sisters.*

*My best friends:*

*(Naïma ,Linda ,Ahlem ,Mounira ,Radia).*

*Everyone who contributed to my success.*

*Siham*

# *Acknowledgements*

*First of all we thank the Almighty **Allah**, whose Grace enabled us to Continue this work and overcome all difficulties and patience to complete this modest work and our **prophet Mohammed** (peace and blessings of Allah be upon him) who invites us to science and knowledge.*

*After that, we make a point of profoundly thanking to our supervisor **Pr. Almi kenza**, Professor at the Department of sciences of matter at Faculty of Exact Sciences and Sciences of Nature and Life in Mohamed Khider University of Biskra.*

*Who granted us the opportunity to be one of her students and to do this research, we are indebted to her for her guidance, suggestions, and valuable remarks and for her help, support and encouragement. She has been a great support on all fronts.*

*We'd dress our sincere thanks to **Pr. Lakel Said**, for the honor that makes to us by accepting the presidency of this jury.*

*We're grateful to **Pr. Boudour Bariza**, who agreed to accept to belong to the jury and to examine my work.*

*Our greatest indebtedness goes to our **Fathers** and **Mothers** for their Valuable advice, all our Families and to our Friends for their endless support.*

*We'd like to thank many people have inspired, guided, helped, and laughed with during the **5 years** we spent at The **University of Biskra**.*

*Finally, we wish to address our thanks to all the teachers and students of the department of sciences of matter especially the **Professor of physics**, everyone by his name.*



*Table Of contents*

# *Table of contents*

Dedication Linda	
Dedication Siham	
Acknowledgements	
Table of contents .....	i
List of figure .....	v
List of Tables .....	vii
General Introduction .....	1
References of General Introduction .....	3

## ***Chapter I: Bibliographic Study on TCO Thin Films and Deposit Techniques.***

1. Introduction: .....	4
2. Generalities about thin films: .....	4
2.1. Definition of thin films: .....	4
2.2. Thin films growth mechanisms: .....	4
3. The technique of depositing thin films: .....	4
4. Sol-Gel method: .....	5
4.1. Definition: .....	5
4.2. Principle: .....	5
4.3. Chemical reactions in the Sol-Gel process: .....	7
4.4. Sol-Gel transition: .....	7
4.5. Advantages and Disadvantages of Sol-Gel method: .....	8
4.5.1. The advantages: .....	8
4.5.2. The disadvantage.....	8
4.6. Techniques of deposition: .....	9
4.6.1. Spin-Coating technique: .....	9
4.6.2. Dip-Coating technique: .....	9
4.6.3. Spray pyrolysis technique: .....	10

4.6.4. Ultrasonic spray technique: .....	11
4.6.5. Spray pneumatic technique: .....	11
5. Transparent Conducting Oxide (TCO): .....	12
5.1. Definition of TCOs: .....	12
5.2. TCOs Materials: .....	12
5.3. Physical properties of TCOs: .....	13
5.3.1. Electrical conductivity: .....	13
5.3.2. Optical properties .....	14
5.4. Applications of TCOs: .....	15
6. Generalities about copper oxide: .....	16
6.1. The choice of copper oxide: .....	16
6.2. Copper oxides Cu <sub>2</sub> O and CuO: .....	16
6.2.1. Cu <sub>2</sub> O oxide (cuprite): .....	16
6.2.2. Structural properties: .....	16
6.2.3. CuO oxide (tenorite): .....	18
6.2.3.1. Physical and chemical properties of cupric oxide (CuO): .....	19
6.2.3.2. Crystal structure of cupric oxide thin films: .....	19
6.2.3.3. Structural properties: .....	21
6.2.3.4. Optical properties: .....	21
6.2.3.5. Electrical properties: .....	22
6.2.3.6. Electronic transmission properties CuO: .....	23
6.3. Application of copper oxide: .....	24
7. Previous work on copper oxide CuO: .....	24
References of Chapter I: .....	26

## ***Chapter II: Elaboration and Characterization of CuO Thin Films.***

1. Introduction: .....	29
2. Chemical components used in the preparation of solutions: .....	29
2.1. Precursor: .....	29

2.2. The source of dopants: .....	30
2.3. The solvent: .....	30
2.4. Catalyst: .....	31
3. Experimental procedure: .....	32
3.1. Preparation of Substrates: .....	32
3.1.1. Choice of substrates: .....	32
3.1.2. Substrates cut: .....	32
3.1.3. Substrates Cleaning Process: .....	33
3.2. Preparation of solutions: .....	34
3.3. Deposition of Thin Films: .....	35
3.3.1. Spin coating method: .....	35
3.3.2. Heat treatment: .....	36
3.3.3. Drying thin films: .....	36
3.3.4. Annealing Thin Films: .....	37
3.3.5. Characterization Techniques of Thin Films: .....	40
3.4. Structural characterization: .....	40
3.4.1. X-Ray Diffraction (XRD): .....	40
3.4.1.1. Principle of analysis: .....	40
3.4.1.2. The apparatus used in this study: .....	42
3.4.1.3. Determination of the inter-reticular distances And the cell parameters: .....	43
3.4.1.4. Determination of the Grain Size: .....	43
3.4.1.5. Determination of constraints: .....	44
3.4.1.6. Determination of Dislocations' density: .....	45
3.5. Optical characterization: .....	45
3.5.1. Ultraviolet-visible spectroscopy (UV- VIS): .....	45
3.5.2. The Thickness of the Film: .....	47
3.5.2.1. The Approximate Gravimetric Method: .....	47
3.5.2.2. Measurement of thickness by interference fringe method: .....	47

3.5.3. Determination of the absorption coefficient: .....	48
3.5.4. Determination of the optical gap: .....	49
3.5.5. Determination of The disorder (the energy of Urbach): .....	50
3.5.6. Determination of the refractive index: .....	51
References of Chapter II: .....	52

### ***Chapter III: Results and Discussion.***

1	Introduction: .....	55
2	Optical Properties of Mg Doped CuO Thin Films: .....	55
	2.1. Transmittance spectra: .....	55
	2.2. Absorbance spectra: .....	56
	2.3. The absorption coefficient: .....	56
	2.4. The optical Gap (E <sub>g</sub> ): .....	57
	2.5. The Disorder (Urbach energy): .....	59
	2.6. The reflection: .....	61
	2.7. The extinction coefficient K: .....	62
	2.8. The refractive index n: .....	63
	References of Chapter III: .....	64
	General Conclusion .....	65



*List of Figure*

# List of figures

Figure	Title	Page
<b>Chapter I: Bibliographic Study on TCO Thin Films and Deposit Techniques.</b>		
I.1	Classification of thin film deposition techniques.	4
I.2	Sol-gel process.	5
I.3	The Sol-Gel transition.	6
I.4	The process of Spin coating technique.	8
I.5	Spray pyrolysis process.	9
I.6	Spray pyrolysis process.	9
I.7	Ultrasonic spray process.	10
I.8	Spray pneumatic process with a gun.	11
I.9	Optical window schema for Transparent Conducting Oxides.	13
I.10	Some applications of TCOs.	14
I.11	Crystal structure of Cu <sub>2</sub> O.	16
I.12	a) Unit cell of CuO. b) Crystal structure of CuO shown by four unit cells.	19
I.13	Transmittance spectra of CuO thin films prepared by spray pyrolysis technique.	21
I.14	Band structure of CuO calculated using the DFT+U method. The Fermi level is set at 0 ev.	22
I.15	Some applications of CuO thin films.	23
<b>Chapter II: Elaboration and Characterization of CuO Thin Films.</b>		
II.1	Copper acetate.	30
II.2	Magnesium acetate.	30
II.3	Ethanol.	31
II.4	HCL.	31
II.5	The substrates.	32
II.6	Substrates cut .	33
II.7	Substrats Cleaning Process.	33
II.8	Digital scale.	34
II.9	Magnetic stirrer.	34
II.10	The solution.	34
II.11	The spin coating machine.	35
II.12	The drying oven.	36
II.13	The annealing furnace.	37
II.14	Flow chart of sol-gel method (spin coating) for preparation of CuO thin films.	39
II.15	Diffraction of X-rays by a crystal according to Bragg's law.	41
II.16	The x-ray diffractometer used in the analysis of x-ray diffraction of the samples.	42
II.17	Diagram of an X-ray Diffractometer.	42
II.18	Determination of $\beta$ .	44
II.19	The principle of operation of UV-visible.	46

<b>II.20</b>	Ultraviolet-visible spectrophotometer (LAMBDA 25).	<b>46</b>
<b>II.21</b>	The physical constants used in the calculations.	<b>47</b>
<b>II.22</b>	Method of interference fringes to determine the thickness.	<b>48</b>
<b>II.23</b>	Determining the energy gap $E_g$ .	<b>50</b>
<b>II.24</b>	Determination of the disorder by extrapolation from the variation of $\ln(\alpha)$ as a function of $h\nu$ .	<b>51</b>
<b>Chapter III: Results and Discussion.</b>		
<b>III.1</b>	Optical transmittance spectra of Mg CuO thin films as a function of wavelength.	<b>55</b>
<b>III.2</b>	Optical absorbance spectra of Mg CuO thin films as a function of wavelength.	<b>56</b>
<b>III.3</b>	The absorption coefficient of Mg doped CuO as a function of the wavelength.	<b>55</b>
<b>III.4</b>	The variation of $(\alpha h\nu)^2$ as a function of $h\nu$ for each Doping percentage.	<b>58</b>
<b>III.5</b>	Effect of doping ratio on the gap band $E_g$ .	<b>59</b>
<b>III.6</b>	Variations of $\ln(\alpha)$ as a function of $h\nu$ .	<b>60</b>
<b>III.7</b>	Effect of doping ratio on the disorder energy $E_{00}$ .	<b>61</b>
<b>III.8</b>	Optical reflection spectrum of Mg doped CuO films as a function of wavelength.	<b>62</b>
<b>III.9</b>	Variation of the extinction index as a function of the wavelength.	<b>62</b>
<b>III.10</b>	The refractive index profile of Mg doped CuO films.	<b>66</b>



*List of Tables*

# List of Tables

Table	Title	Page
<b>Chapter I: Bibliographic Study on TCO Thin Films and Deposit Techniques.</b>		
I.1	TCO Materials.	13
I.2	Lists of crystallographic, elastic, and electronic properties of Cu <sub>2</sub> O.	18
I.3	Physical properties of CuO.	19
I.4	Crystallographic properties of CuO.	20
<b>Chapter II: Elaboration and Characterization of CuO Thin Films.</b>		
II.1	The physical and chemical properties of copper acetate.	30
II.2	The physical and chemical properties of magnesium acetate.	30
II.3	The physical and chemical properties of Ethanol.	31
II.4	The physical and chemical properties of HCL.	31
II.5	The parameters used for depositing our thin films.	38
<b>Chapter III: Results and Discussion.</b>		
III.1	Optical gap values.	59
III.2	Disorder's (Urbach energy) values.	61



*General Introduction*

### **General Introduction:**

Transparent conducting oxides (TCOs) are known as materials that show both transparent and conducting properties, and their films are utilized in flat panel displays, solar cells and electroluminescent devices as transparent electrodes as reviewed in [1, 2, 3]. Two main properties are required to belong to TCOs semiconductors, the transparent property which means a high optical transmission in the visible range, and that requires an energy gap larger than 3.3 eV. Then the conducting property which signify a high electrical conductivity in the range of 1 to  $10^4 \text{ S cm}^{-1}$  [4, 5, 6, 7].

Mono-oxide nature of copper oxide (CuO) makes it very important semiconductors for practical application and other essential investigation. Copper oxide (CuO) draw attention of many researcher for its semiconducting properties due to the presence of Transition Metal Oxides, a p-type semiconductor material with a narrow band gap in bulk (1.2 eV) [8]. High electron-hole pair recombination and high resistivity CuO a nanostructure limits its applications. To overcome this problem, some surface modifications to be introduced by varying its size and shape via preparing some high-quality nanostructures in a definite area. Another alternative is the doped CuO with other suitable materials like Fe, Mn, Zn, W and Mg. Among them, Mg is considered the most promising as dopant element because of compatibility and surface modification. Also, Mg was considered to be a dopant material due to the resemblance of ionic radii of  $\text{Cu}^{+2}$  and  $\text{Mg}^{+2}$ . These modifications need to prepare these materials with high control, desirable size and shape [9].

This work focuses focuses on the development and characterization of magnesium-doped copper oxide (CuO: Mg) thin films. The purpose of this is the improvement of the structural and optical properties of CuO thin films during magnesium doping. To obtain Mg doped CuO thin films deposited on glass substrate, Sol-Gel (spin-coating) was used, and the motivation of choosing the sol-gel spin-coating deposition technique is its simplicity.

The work described in this dissertation is organized in general introduction, and general conclusion, and three chapters presented as follows:

**In the first chapter** we will talk briefly about thin films and about researches carried out on conductive transparent oxides (TCOs), especially about copper oxide CuO thin

## *General Introduction*

---

films, their properties and their most important applications in various technological areas.

In **the second chapter** we present the different steps followed for the deposition of Mg doped CuO thin films on a glass substrate by the sol-gel process, using the spin coating technique. We will present the experimental details and we describe the various methods adopted to characterize elaborated thin films (structural, optical) used in this study.

**The third chapter** is devoted to presentation of the experimental results obtained during this work namely optical (UV-VIS) property of the elaborated thin films as well as their discussion and interpretation.

At last, we conclude our study by a **general conclusion** about the main results obtained in this work.



# *Bibliography*

- [1]: D.S. Ginley, H. Hosono, D.C. Paine: Handbook of Transparent Conductors (Springer, Berlin 2011).
- [2]: D.S. Ginley, C. Bright: Transparent conducting oxides, MRS Bulletin 25, 15 (2000).
- [3]: H. Hosono: Thin Solid Films 515, 6000 (2007).
- [4]: K. Ellmer: Nat. Photonics 6, 809 (2012).
- [5]: C.G. Granqvist: Sol. Energy Mater. Sol. Cells 91, 1529 (2007).
- [6]: P.D.C. King, T.D. Veal: J. Phys.: Condens. Matter 23, 334214 (2011).
- [7]: S. Calnan, A.N. Tiwari: Thin Solid Films 518, 1839 (2010).
- [8]: J. wook Ha, J. Oh, H. Choi, H. Ryu, W. J. Lee, and J. S. Bae, “Photoelectrochemical properties of Ni-doped CuO nanorods grown using the modified chemical bath deposition method”, J. Ind. Eng. Chem., vol. 58, pp. 38–44, 2018.
- [9]: L. B. Luo et al, “One-dimensional CuO nanowire: synthesis, electrical, and optoelectronic devices application”, Nanoscale Res. Lett., vol. 9, no. 1, pp. 1–8, 2014.

**Chapter I:**

***Bibliographic Study on TCO Thin  
Films and Deposit Techniques***

## **1 Introduction:**

In this chapter, we will talk briefly about thin films and TCOs, especially about copper oxide CuO thin films, their properties and their most important applications in various technological areas.

## **2 Generalities about thin films:**

### **2.1 Definition of thin films:**

Thin films are layers of material ranging from fractions of a nanometre to several micrometres in thickness. The controlled synthesis of materials as thin films is a fundamental step in many applications. Thin films are primarily used in the manufacturing of electronic components such as photovoltaic cells because of their insulating or conductive properties, for the protection of objects to improve mechanical properties and resistance; for instance calf chromium plating decorative coatings (example of gilding) or changing the reflective power of surfaces (anti-reflective lenses or mirrors), It is also being applied to pharmaceuticals, via thin-film drug delivery. A stack of thin films is called a multilayer.

### **2.2 Thin films growth mechanisms:**

Thin films growth takes place in several stages:

- ✚ The arrival and adsorption of atoms (or molecules) on the surface of the substrate.
- ✚ The surface diffusion of atoms.
- ✚ Interaction between deposited atoms to form stable bonds.
- ✚ The nucleation of the layer.
- ✚ The growth in the volume.
- ✚ The propagation of atoms on the surface of the substrate.

## **3 The technique of depositing thin films:**

The methods of preparing thin films can be divided essentially into two main groups, namely, physical and chemical methods. These methods are shown in Figure (I.1).

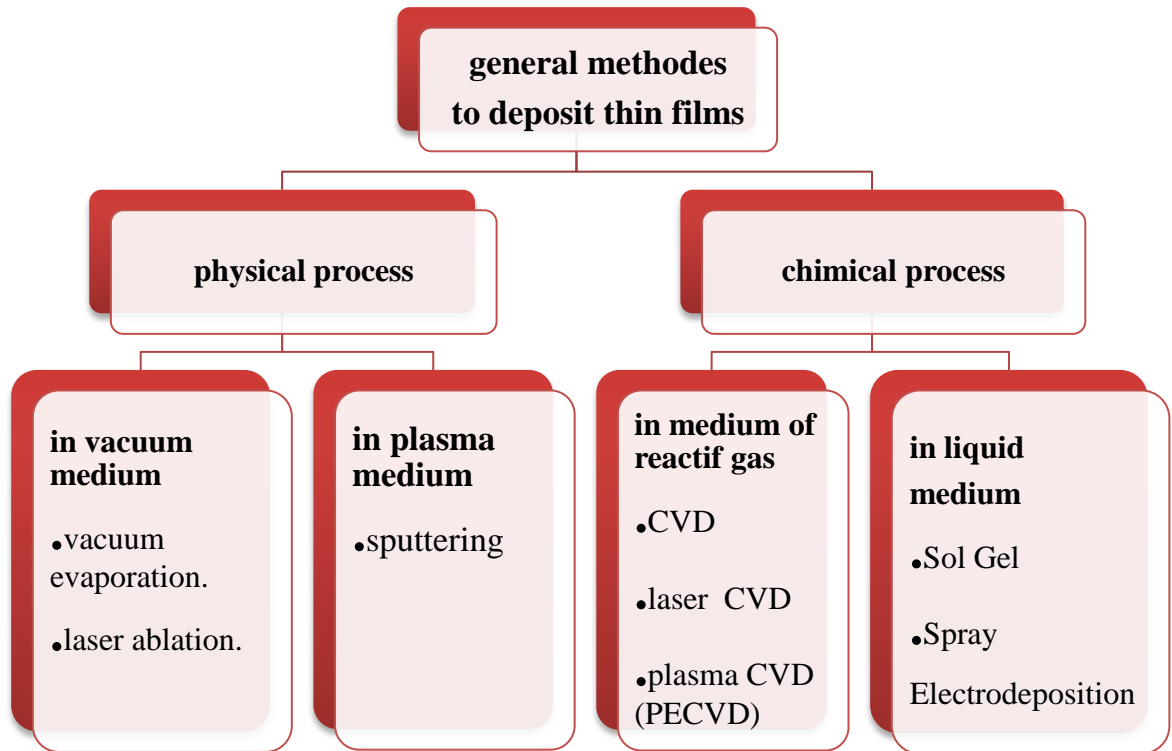


**Figure (I.1):** Classification of thin film deposition techniques[1].

## 4 Sol-Gel method:

### 4.1 Definition:

The sol-gel is a method for producing solid materials from small molecules. The process involves the conversion of monomers into a colloidal solution (sol) that acts as the precursor for an integrated network (or gel) of either discrete particles or network polymers. Typical precursors are metal alkoxides.

### 4.2 Principle:

The sol-gel is a low-temperature method of synthesizing organic material or synthesizing organic and inorganic materials [1]. It is also a simple method to produce high quality and large area thin films compared to other technique [2]. The meaning of «sol-gel» originated from “sol” indicating the evolution of inorganic networks through the formation of a colloidal suspension and (gel) corresponding to the gelation of the sol to form a network in a continuous liquid phase. The sol-gel method is widely employed to deposit thin films, to synthesize nonmaterial and ceramics[3].

The sol-gel process of thin films includes the following steps:

- Preparation of a sol.
- Gelling the sol on a substrate.
- Drying and densification by sintering [4].

-There are two ways of sol-gel synthesis :

➤ **Modality inorganic or colloidal:** Colloidal methods are simple and well-established chemistry precipitation processes . Under the control temperature and pressure, solutions of different ions are mixed to form insoluble precipitates. It is an important type of synthesis approach for semiconductor . The colloidal method is used to form nanosized particles within a continuous fluid solvent matrix. In this method, the monodispersed system is found to have a high energy state, which is equivalent to the free energy required to fabricate the increased surface area.

➤ **Modality organic or polymeric route:** obtained from metallic alkoxides in organic solutions. This route is relatively expensive but allows fairly easy control of the grain size. In both cases, the reaction is initiated by hydrolysis allowing the formation of MOH groups and then happens the condensation allowing the formation of M-O-M bonds or hydroxo (M-OH-M) bridges, and so generating metal-oxo or metal-hydroxo polymers in solution. The typical steps involved in sol-gel processing are shown in the schematic diagram below figure (I.2).

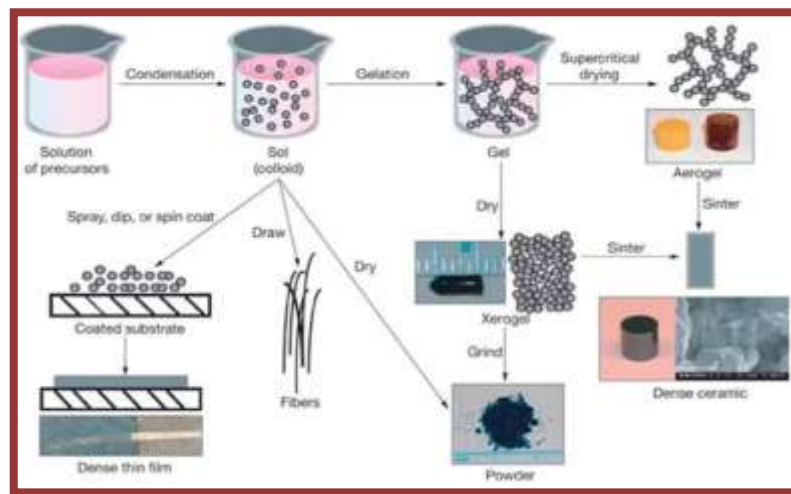


Figure (I.2): Sol-gel process[4].

### 4.3 Chemical reactions in the Sol-Gel process:

This method makes use of molecular precursors in solution, which gradually transformed into a network of oxides by polymerization reactions. Generally, the starting solution is constituted by a metal precursor Alcoyle of the formula:  $M(OR)_n$  where, M: is an n-valent metal and R an alkyl string ( $C_nH_{2n-1}$ ) to which a solvent is added (a catalyst and sometimes water). Namely, the chemical nature of the solvent and precursor dictates the appropriate catalyst [5-6]. The predominant reactions can be divided into two categories [7-8]:

- ✓ Hydrolysis reactions.
- ✓ Condensation reactions.

### 4.4 Sol-Gel transition:

The sol-gel transition (also known as gelatin) is simply a change from a liquid state to a gel state. In the liquid state, components dispersed in the liquid are relatively free to move about. In the gel state, these subunits bond together to form a network extending throughout the whole substance (see figure (I.3)). The network gives the material elasticity.

The composition of the subunits and the bonds between them strongly affect the properties of the gel.M

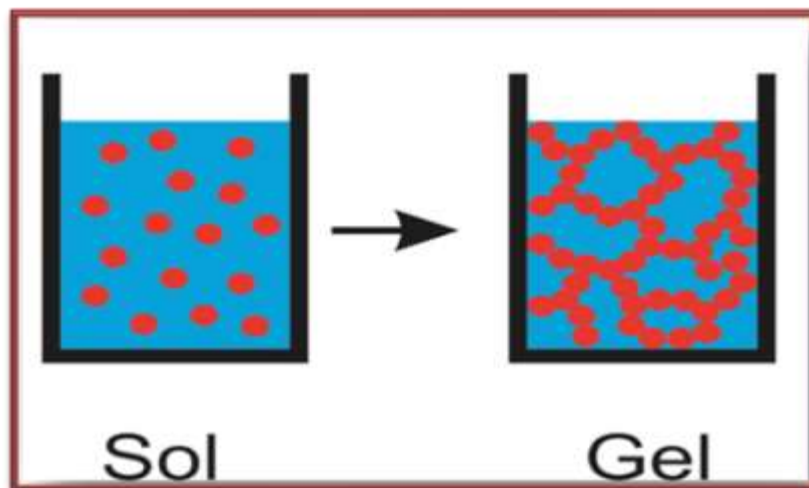


**Figure (I.3):** The Sol-Gel transition.

## **4.5 Advantages and Disadvantages of Sol-Gel method:**

### **4.5.1 The advantages:**

The advantages of this method are manifold making it a coveted method ,we quote here their main advantages :

- ✓ Simplicity of the process and speed of execution .
- ✓ Simultaneously coating both sides of the substrate in a single operation (dip coating) and the ability to form multilayer.
- ✓ Feasibility of multicomponent coatings by simply mixing the corresponding alkoxy in the starting solution.
- ✓ Ability to optimize the morphology of the films based on re- searched applications.
- ✓ Ability to produce thin layers of inorganic oxides at low temperature on heat sensitive substrates.
- ✓ Possibility of making organo hybrid materials as thin or monolithic layers with specific properties.
- ✓ Doping facilitated in large quantities.

### **4.5.2 The disadvantages:**

The main disadvantages are:

- ✓ Cost of high - alkoxide precursors.
- ✓ Manipulation of a large amount of solvents.
- ✓ the major drawback is the low thickness of the layers , so one must perform several. steps of depositing and drying to obtain a thickness of several hundred nanometers,which increases the risk of cracking as the first deposited layers undergo all successive drying which increases the risk of short circuit when the electrical tests [9].

## 4.6 Techniques of deposition:

Several techniques can be used for the deposition of thin films on a given substrate: Spin-Coating, Dip-Coating, spray pyrolysis, spray ultrasonic and spray pneumatic.

### 4.6.1 Spin-Coating technique:

The solution is placed on the substrate and then the substrate is rotated to spread the solution by centrifugal force. At this stage, gas blowing toward the substrate during rotation can be used. The film thickness can be controlled by varying rotation speed, rotation time and coating solution viscosity. The used solvent is usually volatile and simultaneously evaporates. The machine used for spin coating is called a spin coater or spinner. A coating process using spin coater or spinner is illustrated in Figure (I.4) [3].

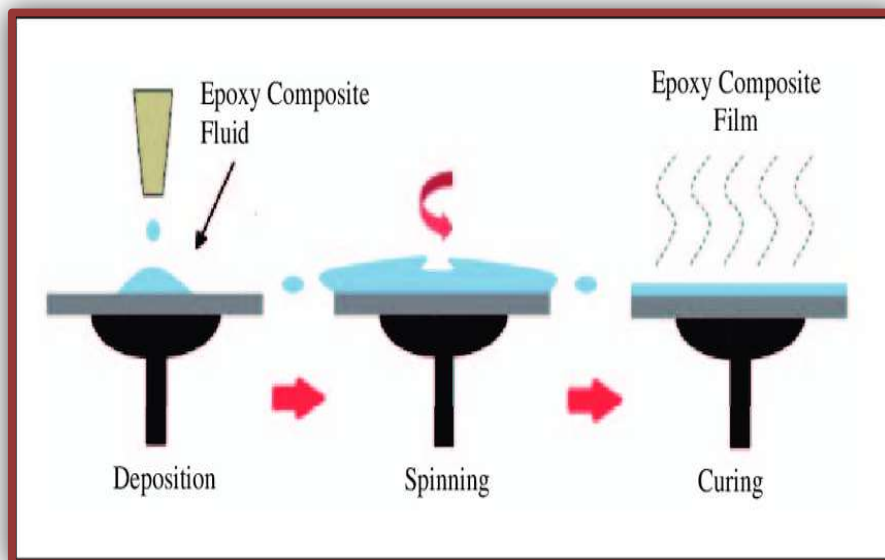


**Figure (I.4):** the process of Spin coating technique.

### 4.6.2 Dip-Coating technique:

The dip-coating process is one of the commonly used liquid-phase deposition methods for the formation of thin films. In dip-coating technique, a substrate is dipped into a liquid coating solution and then is withdrawn from the solution at a controlled speed. Coating thickness generally increases with faster withdrawal speed. The thickness is determined by the balance of forces at the stagnation point on the liquid surface. A faster withdrawal speed pulls more fluid up onto the surface of the substrate before it has time to flow back down into the solution. The thickness is primarily affected by fluid viscosity, fluid density, and surface tension.

After the liquid component of this solution is dried, a solid thin film remains on the substrate.

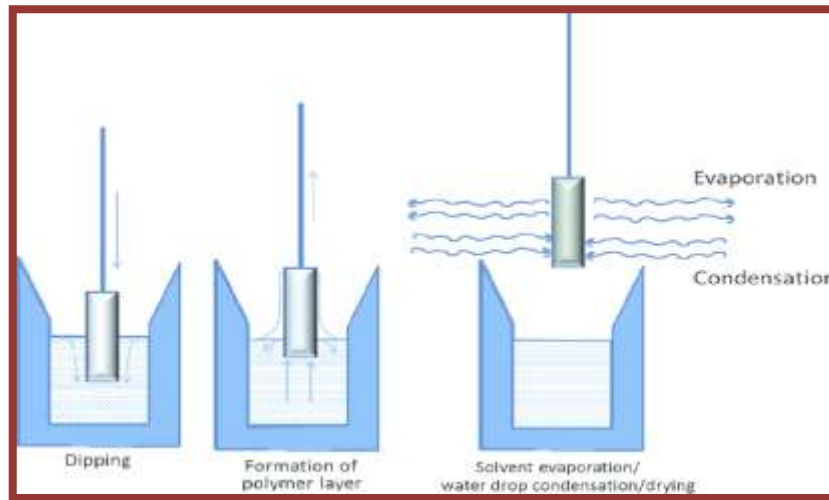


**Figure (I.5):** Spray pyrolysis process.

#### 4.6.3 Spray pyrolysis technique :

The spray pyrolysis is a process in which a thin film is deposited by spraying a solution on a heated surface, where the constituents react to form a chemical compound. The chemical reactants are selected so that all the products other than the desired compound volatilize at the temperature of deposition. As it is shown in figure (I.6).

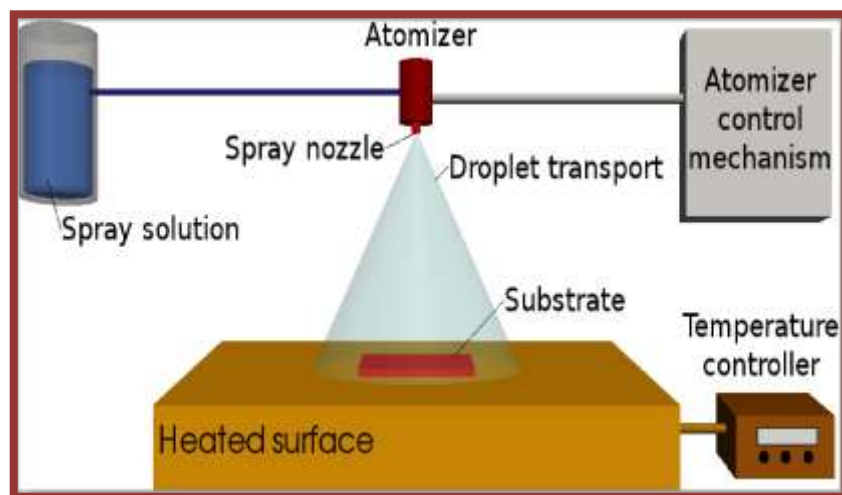


**Figure (I.6):** Spray pyrolysis process.

#### 4.6.4 Ultrasonic spray technique:

Ultrasonic spray technique uses sound vibrations to convert the coating solution into a mist of very small droplets shown in the figure(I.7) below . This allows a more

homogeneous distribution of the droplets, and this is why is sometimes preferred to spray coating using air [1]. The resulting droplets size is in the micrometre range, leading to a good reproducibility of the coatings.

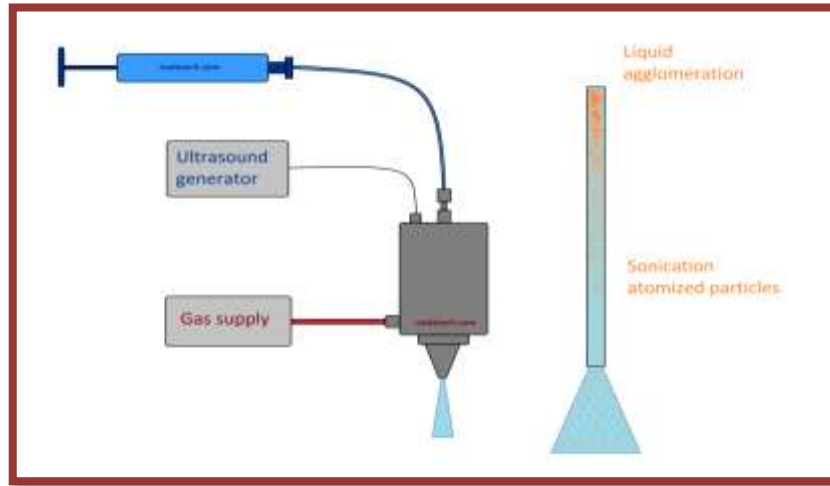


**Figure (I.7):** Ultrasonic spray process.

#### **4.6.5 Spray pneumatic technique :**

Spray painting is a painting technique where a device sprays a coating (paint, ink etc.) through the air onto a surface. Also known as aerosol paint, is paint that's stored in a pressurized container and dispensed using a valve to release a mixture of paint and a propellant, usually pressurized gas or compressed air. The result is a fine, even mist that is easily applied to a variety of surfaces. Generally, Air gun spraying uses larger equipment. It is typically used for covering large surfaces with an even coating of liquid. Spray guns can be either automated or hand-held and have interchangeable heads to allow for different spray patterns.

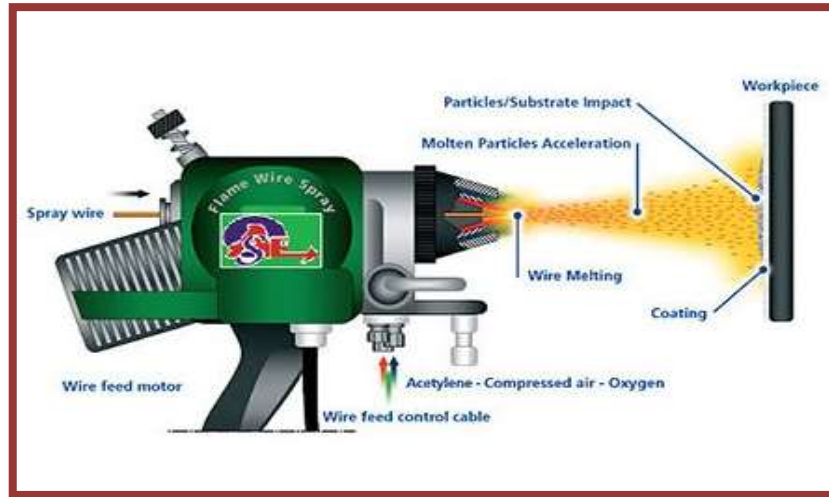


**Figure (I.8):** Spray pneumatic process with a gun.

## 5 Transparent Conducting Oxide (TCO):

### 5.1 Definition of TCOs:

Transparent conductive oxides (TCO) are doped metal oxides used in optoelectronic devices such as flat panel displays and photovoltaics (including inorganic devices, organic devices, and dye-sensitized solar cell). Most of these films are fabricated with polycrystalline or amorphous microstructures.

Current transparent conducting oxides used in industry are primarily n-type conductors, meaning their primary conduction is as donors of electrons. This is because electron mobilities are typically higher than hole mobilities, making it difficult to find shallow acceptors in wide band gap oxides to create a large hole population. Suitable p-type transparent conducting oxides are still being researched, though the best of them are still orders of magnitude behind n-type TCOs. The lower carriers' concentration of TCOs with respect to metals shift their plasmonic resonance into the NIR and SWIR range[10].

### 5.2 TCOs Materials:

A large number systems has been studied as a candidate material for a TCO [11].Table (I.1) lists the commonly used TCO host materials and corresponding dopants. These include binary oxides, ternary oxides and also multi-component oxides.

Table (I.1): TCOs Materials .

Material	Dopant or compound
$\text{In}_2\text{O}_3$	Sn, Ge, Mo, F, Ti, Zr, Hf, Nb, Ta, W, Te.
$\text{SnO}_2$	Sb, F, As, Nb, Ta.
$\text{ZnO}$	Al, Ga, B, In, Y, Sc, F, V, Si, Ge, Ti, Zr, Hf.
$\text{CdO}$	In, Sn.
$\text{ZnO-SnO}_2$	$\text{Zn}_2\text{SnO}_4$ , $\text{ZnSnO}_3$ .
$\text{ZnO-In}_2\text{O}_3$	$\text{Zn}_2\text{In}_2\text{O}_5$ , $\text{Zn}_3\text{In}_2\text{O}_3$ .
$\text{In}_2\text{O}_3\text{-SnO}_2$	$\text{In}_4\text{Sn}_3\text{O}_{12}$ .
$\text{CdO-SnO}_2$	$\text{Cd}_2\text{SnO}_4$ , $\text{CdSnO}_3$ .
$\text{CdO-In}_2\text{O}_3$	$\text{CdIn}_2\text{O}_4$ .
$\text{GaInO}_3$ , $(\text{Ga, In})_2\text{O}_3$	Sn, Ge.
$\text{CdSb}_2\text{O}_6$	Y.
$\text{ZnO-In}_2\text{O}_3\text{-SnO}_2$	$\text{Zn}_2\text{In}_2\text{O}_5\text{-In}_4\text{Sn}_3\text{O}_{12}$ .
$\text{CdO-In}_2\text{O}_3\text{-SnO}_2$	$\text{CdIn}_2\text{O}_4\text{-Cd}_2\text{SnO}_4$
$\text{CuXO}_2$	X=Al, Ga, In.
$\text{ZnXO}_4$	X=Al, Ga, Co, Rh, Ir.

### 5.3 Physical properties of TCOs:

#### 5.3.1 Electrical conductivity:

TCOs are wide bandgap ( $E_g$ ) semiconducting oxides, with conductivity  $\rho$  in the range of  $10^2 - 1.2 \times 10^6$  (S). The conductivity is due to doping either by oxygen vacancies or by extrinsic dopants. In the absence of doping, these oxides become very good insulators, with  $\rho > 10^{10}$   $\Omega\text{cm}$ . Most of the TCOs are n-type semiconductors. The electrical conductivity of n-type TCO thin films depends on the electron density in the conduction band and on their mobility, the electrical conductivity of p-type TCO thin films depends on the hole density in the valance band and on their mobility.

Electrical parameters depend on the mechanisms by which the carriers are scattered by lattice imperfections, such as lattice scattering, ionized impurity scattering, neutral impurity scattering, electron-electron scattering and electron-impurity scattering. On the other hand; grain boundary scattering plays an important role in polycrystalline thin films having small grain size [12].

### 5.3.2 Optical properties:

To act as transparent current collectors or as transparent hot-mirror coatings, the TCO films must possess a high metal-type conductivity and must be transparent (colourless) in the visible. Besides, TCOs with high resistivity are required for some specific applications such as transparent micro-furnaces. These different characteristics are achievable by carefully controlling both the electrical conductivity and the «optical window» of the electrodes Shown in Figure (I.9) [13].

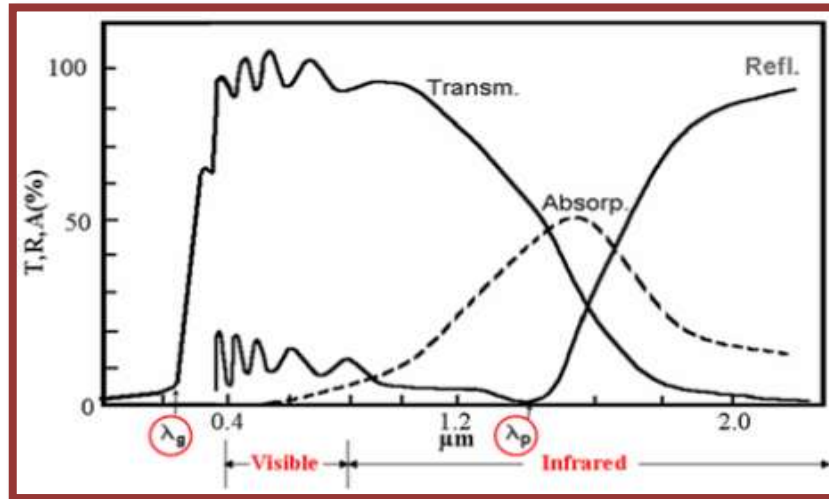


**Figure (I.9):** Optical window schema for Transparent Conducting Oxides[13].

The energy of excitation  $\Delta E$  is related to the absorbed photon frequency based on the electron transitions equation (I.1):

$$\Delta E = h\nu \quad (\text{I.1})$$

As shown in Figure (I. 9): the optical window is delimited by two cutting wavelengths  $\lambda_g$  and  $\lambda_p$ .

The first wavelength,  $\lambda_g$ , separates the absorption zone in the ultraviolet from the transparent zone in the visible. It corresponds to the threshold of inter-band absorptions and it is correlated to the optical band-gap,  $E_g$ , according to for the equation(I.2):

$$E_g = \frac{hc}{\lambda_g} \geq 3eV \quad (\text{I.2})$$

Where:

- ✓  $h$  is Planck's constant.
- ✓  $c$  is the speed of light.

The second wavelength,  $\lambda_p$  (generally called plasma wavelength), corresponds to the front rise of the reflectivity in the IR and accounts for a metallic character of the TCO, it corresponds to intra band absorption in the conduction band of the electrode material, when resonance occurs between the incident electromagnetic radiation and the plasma oscillation of the (quasi) free electrons in the conduction band [13].

$\lambda_p$  depends on the concentration of these electrons in the conduction band ( $N$ ) and on their mobility ( $\mu$ ) according to for the equation (I.3):

$$\lambda_p = 2\pi c \sqrt{\frac{\epsilon_0 \epsilon_\infty \tau}{Ne\mu}} \quad (\text{I.3})$$

Where:

- ✓  $\tau$  is the carrier relaxation time.
- ✓  $\epsilon_0$  is the permittivity of free space.
- ✓  $\epsilon_\infty$  is the high frequency dielectric constant of the involved media [13].

#### 5.4 Applications of TCOs:

For their luminescence properties TCO films have been widely used as a transparent conducting thin-film material to be used in various fields such as solar cells, flat panel displays, smart windows, touch screens, optoelectronic devices, heat mirrors, for liquid crystal displays (LCDs), organic light-emitting diodes (OLEDs), and gas sensors, etc. figure (I.10)[14].

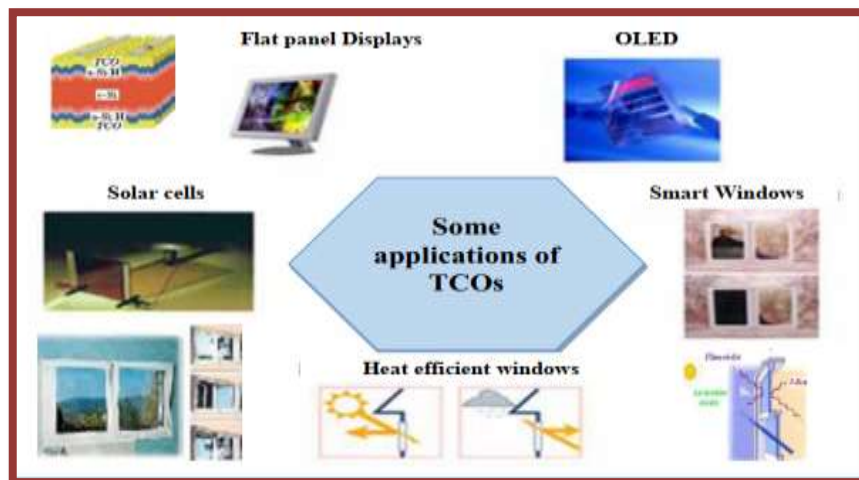


Figure (I.10): Some applications of TCOs [15].

## 6 Generalities about copper oxide:

Copper has two oxidation states +1 and +2, while under special circumstances some compounds of trivalent are also reported. It was shown that this trivalent copper survives not more than a few seconds. Consequently, cuprous oxide ( $\text{Cu}_2\text{O}$ ) and cupric oxide ( $\text{CuO}$ ) are the two stable forms of copper oxide. However, cupric oxide ( $\text{CuO}$ ) phase exhibits a number of interesting properties[16].

### 6.1 The choice of copper oxide:

Cupric oxide ( $\text{CuO}$ ), having a narrow bandgap of (1.2 eV) and a variety of chemophysical properties, is recently attractive in many fields such as energy conversion, optoelectronic devices, and catalyst.

### 6.2 Copper oxides $\text{Cu}_2\text{O}$ and $\text{CuO}$ :

#### 6.2.1 $\text{Cu}_2\text{O}$ oxide (cuprite):

Copper oxide is an inorganic compound with the formula  $\text{Cu}_2\text{O}$ . It is one of the principal oxides of copper, the other being  $\text{CuO}$  or cupric oxide.

#### 6.2.2 Structural properties:

$\text{Cu}_2\text{O}$  crystallizes in a cubic structure with a lattice constant ( $a = 4.2696 \text{ \AA}$ ). The Cu atoms arrange in a fcc sublattice, the O atoms in a cc sublattice. One sublattice is shifted by a quarter of the body diagonal. Cuprous Oxide  $\text{Cu}_2\text{O}$  (see Figure (I.11)) is one of the stable phases of the three well-established copper-oxide compounds (the others are  $\text{Cu}_4\text{O}_3$ ,  $\text{CuO}$ ). It crystallizes in a simple cubic Bravais lattice [17]. The space group is ( $\text{Pn}3\bar{\text{m}}$ ) or  $O_h4$ . Its unit cell contains six atoms, the four copper atoms are positioned in a face-centre cubic lattice (violet balls), the two oxygen atoms are at tetrahedral sites forming a body centre cubic sublattice (black balls). As a consequence, oxygen atoms are fourfold coordinated with copper atoms as nearest neighbours, and copper atoms are linearly coordinated with two oxygen atoms as nearest neighbours and copper atoms are linearly coordinated with two oxygen atoms as nearest neighbors (see Table (I.1) and for resulting crystallographic and physical properties[18]).

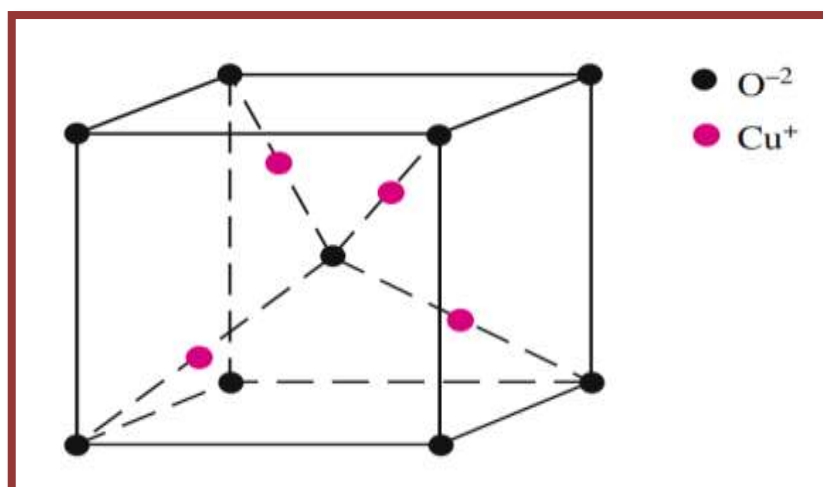


Figure (I.11): Crystal structure of  $\text{Cu}_2\text{O}$  [18].

**Table (I.2):** Lists of crystallographic, elastic, and electronic properties of Cu<sub>2</sub>O[19].

<b>lattice constant</b>	<b>4.2696 ± 0.0010 Å</b>
<b>space group</b>	Pn3 <sup>-</sup> m (224) $O_h^4$
<b>bond length Cu2O</b>	1.849 Å
<b>separation OO</b>	3.68 Å
<b>separation CuCu</b>	3.012 Å
<b>cell volume</b>	(77.833 ± 0.055) 10 <sup>-24</sup> cm <sup>3</sup>
<b>formula weight</b>	143.14
<b>Density</b>	5.749 - 6.140 g/cm <sup>3</sup>
<b>melting point</b>	1235° C
<b>Youngs modulus</b>	30.12 GPa
<b>Shear modulus</b>	10.35 GPa
<b>c11</b>	116.5126.1 GPa
<b>c12</b>	105.3108.6 GPa
<b>c44</b>	12.113.6 GPa
<b>Coefficient of thermal expansion</b>	2.3 × 10 <sup>-7</sup> K <sup>-1</sup> (283K)
<b>Froehlich coupling constant a</b>	0.21
<b>ε(0)</b>	7.11
<b>ε (∞)</b>	6.46
<b>Electron affinity χ</b>	≈3.1eV(300K)
<b>Work function Φ</b>	≈4.84eV(300K)
<b>Deformation potentials</b>	<i>De</i> = 2.4eV <i>Dh</i> = 2.2eV

### 6.2.3 CuO oxide (tenorite):

Copper (II) oxide is an inorganic compound with the formula CuO. A black solid, it is one of the two stable oxides of copper, as a mineral, it is known as tenorite. It is a product of copper mining and the precursor to many other copper-containing products and chemical compounds.

#### 6.2.4 Physical and chemical properties of cupric oxide (CuO):

Pure cupric oxide is black solid with a density of 6.32 g/cm<sup>3</sup> and insoluble in water. It melts above 1134 °C with some loss of oxygen. Table (I.3) regroups some physical and chemical properties of cupric oxide.

**Table (I.3):** Physical properties of CuO[20].

Cupric oxide CuO	
<b>Chemical names</b>	copper (II) oxide Cupric oxide Copper monoxide Copper oxide (CuO) Oxocopper
<b>Molecular formula</b>	CuO
<b>Appearance</b>	black to brown powder
<b>Solubility in water</b>	Insoluble
<b>Molecular mass</b>	79.55 (g/mol)
<b>Density</b>	6.32(g/cm <sup>3</sup> )
<b>melting point</b>	1134 °C
<b>Boiling point</b>	2000 °C
<b>Refractive index</b>	1.4 [21]
<b>Hole effective mass</b>	0.2 m <sup>2</sup> [21]
<b>Hole mobility</b>	0.1-10(cm <sup>2</sup> /Vs) [21]
<b>Magnetic susceptibility(x)</b>	+238.9× 10 <sup>-6</sup> cm <sup>-3</sup> /mol
<b>Refractive index (n<sub>D</sub>)</b>	2.63

#### 6.2.5 Crystal structure of cupric oxide thin films:

Cupric oxide has a more complicated tenorite crystal structure than other oxides of copper. The monoclinic unit cell (space group **C2/2** ) contains four CuO molecules, shown in Figure (I.3). The atoms coordination is that each atom has four nearest neighbours of the other kind. For example, in the (110) plan (as depicted in Figure (I.12)), each **Cu** atom (the turquoise spheres) is linked to four nearest **O** atoms at the corner of an almost rectangular parallelogram. While each **O** atom (the red spheres) is coordinated to four **Cu** atoms in the

form of a disorder tetrahedron. Lattice constants and other crystallographic properties are listed in Table (I.4)[20].

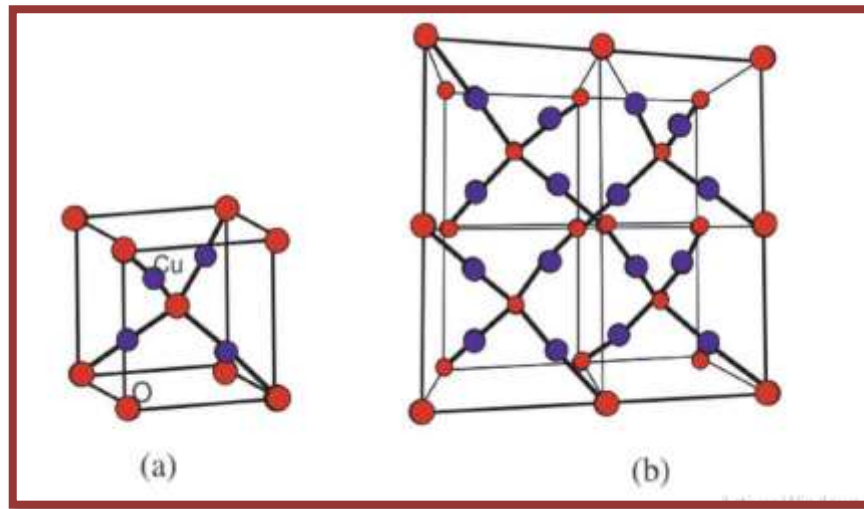


**Figure (I.12):** a) Unit cell of CuO. b) Crystal structure of CuO shown by four unit cells.

**Table (I.4):** Crystallographic properties of CuO [20]:

Crystallographic properties of CuO	
Space group	C2/c
Unit cell	$a = 4,6837 \text{ \AA}$ $b = 3,4226 \text{ \AA}$ $c = 5,1288 \text{ \AA}$ $\beta = 99,548^\circ$ $\alpha, \gamma = 90^\circ$
Cell volume	$81,08 \text{ \AA}^3$
Cell content	4[CuO]
Distances	
Cu-O	1.96 $\text{ \AA}$
Cu-Cu	2.62 $\text{ \AA}$
O-O	2.90 $\text{ \AA}$
Rayons ioniques	$\text{Cu}^{2+} = 0.73 \text{ \AA}$ $\text{O}^{2-} = 1.24 \text{ \AA}$

**6.2.5.1 Structural properties:**

It is well argued that thin film growth is strongly related to the deposition conditions and the used method. Indeed, there is a different deposition technique in which the deposition temperature is one of the main parameters that should be controlled to achieve high films quality.

Meryem and all [20] have compiled effect of substrate, annealing and bath temperatures on the structural properties of CuO thin films deposited by different techniques , they note that the formation of pure Cu<sub>2</sub>O thin films occurs at low temperatures (around 200 °C), while the formation of a pure CuO films requires higher temperature ranged from 300 to 500 °C. However the formation of Cu<sub>2</sub>O<sub>3</sub> phase mixed with other CuO compounds are rarely formed. Obi and all[22] have studied the effect of oxygen percentage on the structural properties of cupric oxide (CuO) thin films and they found the presence of the three different phases of copper oxide thin films namely: Cu<sub>2</sub>O, Cu<sub>4</sub>O<sub>3</sub>, and CuO. The apparition of these phases depended strongly on the oxygen percentage.

The oxidation kinetics depends on many factors such as temperature, oxygen partial pressure, annealing time etc. For CuO thin films elaborated with thermal oxidation, a pure CuO thin film is obtained at higher temperature under oxygen atmosphere, however; at lower temperature a mixture of the various copper oxides are formed. Ezenwa[23] have deposited CuO thin films by chemical bath deposition, he have found that the annealing temperature effect strongly the structural proprieties of the deposited films. The increasing of annealing temperature from 300 to 400°C leads to the change of phases and structure from a mixture of Cu<sub>2</sub>O and CuO phase to formation of pure CuO phase. The same observation is found for the CuO thin films elaborated with sol-gel method[24].

**6.2.5.2 Optical properties:**

The optical properties are a crucial parameter for thin films dedicated to optoelectronic devices. The importance of CuO optical proprieties originated from it is useful applications as an absorber layer in solar cells. This application requires the fulfillment of a high absorption in the visible range of solar spectrum.

Since the deposition technique and the experimental parameters affect the structural properties, the film surface morphology, the optical properties are also altered by

the preparation conditions. Regardless the deposition technique, CuO thin films have a transparency ranged from 0 to 17 %.

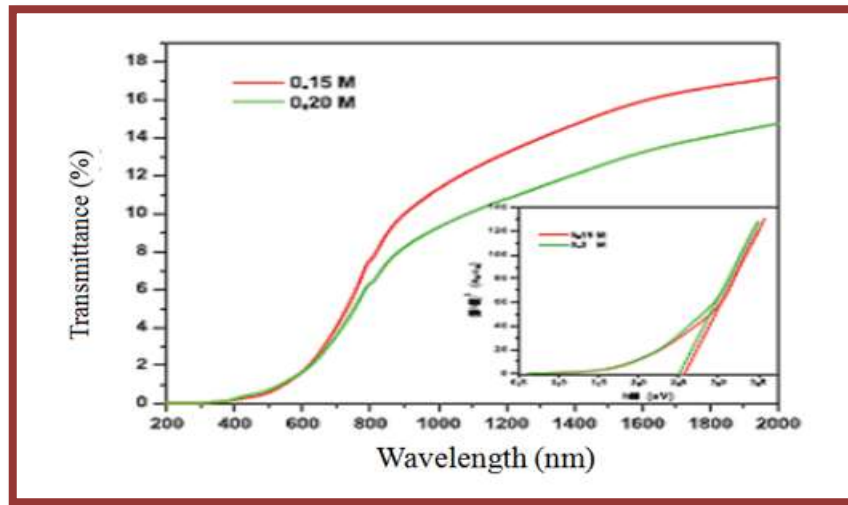


**Figure (I.13):** Transmittance spectra of CuO thin films prepared by spray pyrolysis technique[25].

### 6.2.5.3 Electrical properties:

CuO is classified to be an intrinsically p-type semiconductor, due to the presence of copper vacancies as acceptors being responsible for the hole conduction. The electrical properties of pure CuO are mostly determined by the dominant intrinsic defects, like copper and/or oxygen vacancies. It is well known that copper vacancies are the most dominant defects in a nonstoichiometric cupric oxide due to the copper volatility. copper vacancies give rise to shallow acceptor levels just above the valence band, which leads to p-type behavior[20].

Several experimental studies have been carried out to investigate the deposition techniques and the conditions influence CuO thin films electrical proprieties. The reported dark electrical resistivity of CuO thin films is varied from 10 to  $10^8$  ( $\Omega\text{cm}$ ), depending on the mode of preparation. The measured free carriers concentration and the hole' mobility variation are ranged from  $10^{10}$  to  $10^{16}$   $\text{cm}^{-3}$  and from 10 to 100 ( $\text{cm}^2 \text{V}^{-1} \text{S}^{-1}$ ) respectively.

Any structural changes in thin films alter their electrical properties. These changes include phase change, doping, crystallites size enlargement, grain boundaries and stoichiometry deviation. These variations change the number of charge carriers, their mobility and the transport mechanism which directly affect the resistivity of the films. The

influence of deposition parameters on the resistivity is indirectly due to the influence of these parameters on the stoichiometry of the film and the crystalline structure. The stoichiometric films have a larger resistivity than nonstoichiometric films. In on other hand, it has been found that the resistivity of the film is lower when the grains size is larger [20].

#### 6.2.5.4 Electronic transmission properties CuO:

Cupric oxide (CuO) is a direct band gap semiconductor with the smallest bandgap at the centre of Brillouin zone  $\Gamma$ , as depicted in Figure(I.15) showing the electronic structure of CuO in the monoclinic structure[20]. The calculation using Density Function Theory (DFT) in located density approximation found a bandgap value of (1.251 eV) which is in agreement with the experimental measurements reported at ambient temperature indicating bandgap values in the range 1.2 to 1.9 Ev[22].

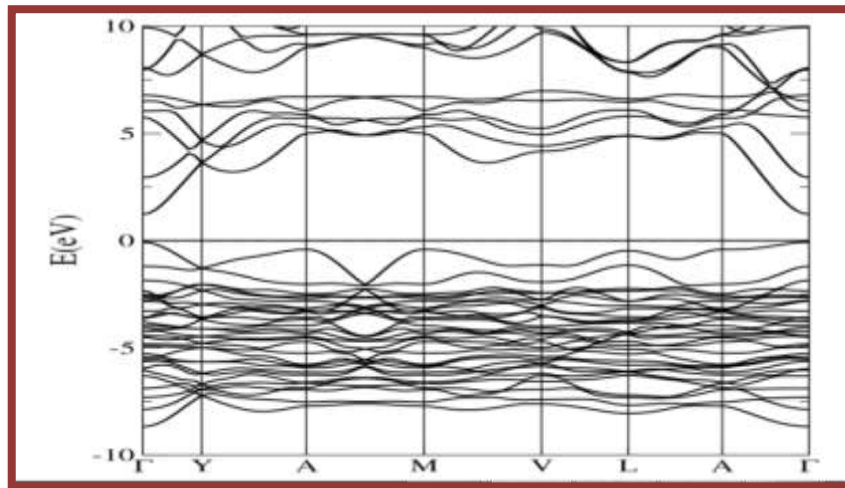


**Figure (I.14):** Band structure of CuO calculated using the DFT+U method. The Fermi level is set at 0 eV[20].

Native point defects are intrinsic to semiconductors; they play an important role in semiconductors electronic properties. Wu and all [26] have calculated the structural relaxation and defect levels induced by various native point defects in CuO. The formation energies of these defects are also calculated for three different types of native point defects: vacancies ( $VCu, VO$ ), antisite defects ( $CuO, OCu$ ) and isolated interstitials ( $Cu_i, O_i$ ). Meryem and all, has found that Cu vacancies ( $VCu$ ) are the most stable defect in CuO due to its lowest formation energy (less than 1.0 eV), indicating that this defect is very easy to form during CuO thin films growth[20].

### 6.3 Application of copper oxide:

CuO is a promising material for various applications due to the abundance of its components in nature, low-cost production, good thermal stability, and electrochemical properties. This combined property enables CuO thin films to be a serious candidate for several applications namely: high-temperature superconductors, solar cells, gas sensors, magnetic storage media, varistors and catalysis, antimicrobial activity, photoelectrochemical cell and Li batteries [20].

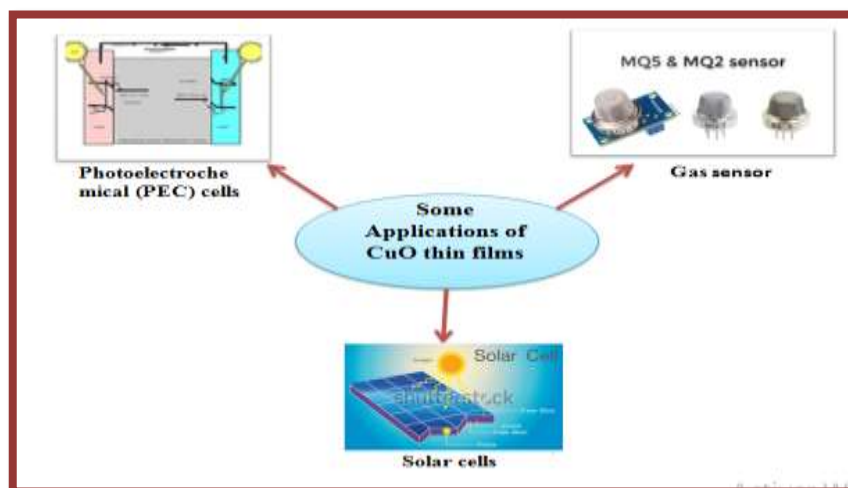


Figure (I.15): Some applications of CuO thin films.

## 7 Previous work on copper oxide CuO:

In recent years, chalcogenide thin films and metal oxide thin films have received much attention. There are two major groups of copper oxide, namely cupric oxide (CuO) and cuprous oxide (Cu<sub>2</sub>O). Below we cite some works among many others that have very interesting applications. Cu<sub>2</sub>O films have cubic structure [Buono-Core et al., 2007; Reddy et al., 2010] with a lattice parameter of (4.27 Å) and direct band gap of (2.1 to 2.6 eV) [Mugwang et al., 2013]. Meanwhile, CuO films are monoclinic crystal structure semiconductor with direct band gap of (1.2 to 2.1 eV). In this work, the preparation of CuO and Cu<sub>2</sub>O films by using various deposition techniques will be investigated and discussed. The resulting films are characterized in terms of optical, compositional, structural, morphological and electrical properties. LITERATURE SURVEY Cu<sub>2</sub>O films are prepared by sol-gel spin coating method on indium tin oxide glass substrate using various additives such as ethylene glycol and polyethylene glycol as described by Halin et al (2014). Cu<sub>2</sub>O films were prepared by electro deposition method onto substrates

using aqueous solution of cupric acid, lactic acid and sodium hydroxide as suggested by Mahalingam et al (2006). Copper oxide in the form of nanoparticles has also been the subject of many research work. Lucile Martin [27] studied the use of copper oxide nanoparticles as conversion materials for micro lithium batteries. The micro batteries at lithium are intended for use for a wide variety of applications such as powering sensors or smart labels, securing smart cards. The main limitation of micro Lithium batteries is their surface capacity, this being mainly limited by the volume capacity of the positive electrode materials, generally less than  $100 \mu\text{Ah}\cdot\text{cm}^{-2}\cdot\mu\text{m}^{-1}$ . Nanoscale particles suspended in a liquid. Eastman et al [28] used CuO nanofluids, 36 nm in diameter with a volume fraction of 5% in water. They achieved a 60% improvement in thermal conductivity, twice higher than the thermal conductivity obtained under the same conditions with  $\text{Al}_2\text{O}_3$  nanoparticles. Lee et al [29] have also used copper oxide nanoparticles to increase the thermal conductivity of nanofluids. They used nanoparticles with a diameter of (18.6 nm) of CuO in water or ethylene glycol. They found that the thermal conductivity of the nanofluid used increases linearly as a function of the volume fraction of the nanoparticles. Li and Peterson [30] carried out experiments using a volume fraction of 10% of (29 nm) diameter CuO nanoparticles in pure water at a temperature of (34.7 ° C). They revealed a 52% improvement in thermal conductivity of the nanofluid. Muath Khairi Hussein Mousa [31], used three different sizes of the nano.



# *Bibliography*

- [1]:T.Pusteln.I.Zielonka, C.Tyszkiewicz, P.Karasinski, B.Pustelny, *opto-electronics review* 14(2), 161-166,2006.
- [2]:L.N.Lau, N.B.I, H.Baqiah, *Applied surface science*, University Kebangsaan Malaysia, Bangi, 43600 Selangor, Malaysia, 2015.
- [3]:P.Dae Hoon, «Optimization of nickel oxide based electrochromic thin films», Doctorate thesis, University Bordeaux 1, France, 2010.
- [4]:O.Tari, «Sol-gel synthesis and characterization of pure and doped transparent and conductive ZnO thin films», Doctorate thesis, University of Naples Federico II, 2013.
- [5]:M .Ebelmen, *Ann. Chim. Phys*, 15, 319, (1845).
- [6]:C. B. Hurd, *Chem. Rev.*, 22, 403 (1938).
- [7]:C.J. Brinker, Sherrer G.W., *Sol-Gel Science*, «The Physic And Chemistry Sol-Gel Processing», Academic Press, San Diego, (1989).
- [8]:H. Cattey, *Thèse De Doctorat*, Université De Franche-Comté, Besançon, (1997).
- [9]:Benelmadjat Hannane, «Elaboration Et Caractérisation Des Composites Dopés Par Des Agrégats Nanométriques De Semi-Conducteurs», *Thèse Magister*, Constantine (2007).
- [10]:Dominici,L.Michelotti,F.Brown, TM, et al.«Plasmon polaritons in the near infrared on fluorine doped tin oxide films». *Optics Express*. 17 (12), 101(55–67), (2009).
- [11]:T. Minami, *Semicond. Sci. Technol*. 20 (2005) S35.
- [12]:I. Saadeddin, « Preparation and characterization of new transparent conducting oxides based on SnO<sub>2</sub> and In<sub>2</sub>O<sub>3</sub>:ceramics and thin films», *Doctorat Thesis*, University Bordeaux I, France , 2007.

- [13]:F.Simonis,M.V.Leij,C.J. Hoogendoorn, «Transparent conducting oxides on polymeric substrates by pulsed laser deposition», solar energy Mater, (1979)
- [14]:I. Saadeddin,«Preperation and Characterization of New Transparent Conducting Oxides Based on SnO<sub>2</sub> and In<sub>2</sub>O<sub>3</sub>: Ceramics and Thin Films», doctorate thesis, University Bordeaux I, 30 Mars 2007.
- [15]:Y.Benkhetta,«L'effet Du Débit De La Solution Sur Les Propriétés Des Couches Minces D'oxyde De Zinc (ZnO) Déposées Par Spray Ultrasonique»,master dissertation, Université Med Khider Biskra ;2003.
- [16]:M.Lamri Zeggar,«Cupric Oxide thin films deposition for gas sensor application», Doctorat thesis, frères Mentouri Constantine 1 university, Algeria, 2016.
- [17]:B.Meyer,A.Polity,D.Reppin,M.Becker,P.Hering,P.Klar,T.Sander,C.Reindl,J.Benz,M Eickhoff, et al., «Binary copper oxide semiconductors: From materials towards devices», physica status solidi (b), vol. 249, no. 8, pp. 1487–1509, 2012.
- [18]:P.YU and M.Cardona,Fundamentals of Semiconductors: Physics and Materials Properties, Springer Berlin Heidelberg, 2013.
- [19]:B. Svensson, S. Pearton, and C. Jagadish, Oxide Semiconductors, ser. Semiconductors and Semimetals. Elsevier Science, 2013.
- [20]:M.Lamri Zeggar, «Cupric Oxide thin films deposition for gas sensor application», Doctorat thesis, frères Mentouri Constantine 1 university, Algeria, 2016.
- [21]:A.Gul , «ZnO and CuO Nanostructures: Low Temperature Growth, Characterization, their Optoelectronic and Sensing Applications»,Linköping University,SE-601 74 Norrköping, Sweden, 2012.
- [22]:P.K.Ooi, S.S. Ng, M.J. Abdullah, H. Abu Hassan, Z. Hassan, Materials Chemistry and Physics 140 (2013) 243.
- [23]:I.A .Ezenwa, Chem. Phys, 50 (2012) 41.
- [24]:S. C. Ray, Solar Energy Materials & Solar Cells 68 (2001) 307.
- [25]:R.Shabu,A.Moses Ezhil Raj,C.Sanjeeviraja,C.Ravi dhas Materials Research Bulletin 68 (2015) 1.

[26]:W. Y. Ching, Y.-N. Xu, K. W. Wong, Phys. Rev. B 40, (1989) 7684.

[27]:L .Martin, « Etude de l'oxyde de cuivre CuO, matériau de conversion en film mince pour microbatteries au lithium, caractérisation des processus électrochimiques et chimiques en cyclage », Thèse doctorat, Université de Pau et des Pays de L'Adour, (2013).

[28]:J.A. Eastman, S.U.S. Choi, S. Li, L.J Thomson, and S. Lee, « Enhanced thermal conductivity through the development of nanofluids ». Materials Research Society Symposium Proceedings, vol. 457, Materials Research Society, Pittsburgh, PA, 3-11, (1997).

[29]:S. Lee, S.U.S. Choi, S. Li, and J.A. Eastman, « Measuring thermal conductivity of fluids containing oxide nanoparticles » , ASME J. Heat Transfer, 121, 280-289, (1999).

[30]:C.H. Li and G.P. Peterson, « Experimental investigation of temperature and volume fraction variations on the effective thermal conductivity of nanoparticle suspensions (nanofluids) », Journal of Applied Physics, 99(8), 084314, (2006).

**Chapter II:**  
***Elaboration and  
Characterization of CuO Thin  
Films***

## **1 Introduction :**

In this chapter we present the different steps followed for the deposition of Mg doped CuO thin films on a glass substrate by the sol-gel process, using the spin coating technique. we will present the experimental details and characterization techniques, which were used in this study. this chapter can be divided into three sections related to the deposition and characterization of the CuO thin films. In the first section, we talk about the chemical components involved in preparing the solution. in the second part, we describe the sample preparation procedure. In the third part, we describe the various methods adopted to characterize CuO thin films.

## **2 Chemical components used in the preparation of solutions:**

The production of magnesium-doped copper dioxide thin films by the sol-gel route can be described in three stages:

- Preparing the solution.
- The deposition.
- Heat treatment of the films developed [1].

The solution used to prepare our magnesium doped CuO samples generally consists of a precursor, a source of dopants, a solvent and a catalyst.

### **2.1 Precursor :**

The quality of the films produced by the sol-gel route depends closely to the property they respond. To allow uniform saturation of the surface, precursors must also be thermally stable at the deposition temperature. Decomposition of the precursor may be the source of saturation incomplete surface or introduction of impurities into the film [2].

The metal-inorganic molecular precursor used in this study is copper acetate (Figure (II.1)) is a chemical compound with the formula  $\text{Cu}(\text{CH}_3\text{COO})_2$ , which is used for the preparation of the solution of the CuO deposit by the sol-gel method. The properties of the precursor are listed in Table (II.1).

**Table (II.1):** The physical and chemical properties of copper acetate.

<b>Chemical name</b>	copper acetate
<b>Molecular formula</b>	$\text{Cu}(\text{CH}_3\text{COO})_2$
<b>Molecular weight</b>	181.63 g/mol
<b>Color</b>	Dark green crystalline solid
<b>Odor</b>	Odorless (hydrate)
<b>Density</b>	1.882 g/cm <sup>3</sup> (hydrate)
<b>Boiling Point</b>	240 °C



**Figure (II.1) :** copper acetate.

## 2.2 The source of dopants :

The source of the doping elements which is magnesium acetate (Figure (II.2)) it was used in the form of a solution. It has the characteristics summarized in Table (II.2):

**Table (II.2):** The physical and chemical properties of magnesium acetate.

<b>Chemical name</b>	magnesium acetate
<b>Molecular formula</b>	$\text{Mg}(\text{CH}_3\text{COO})_2$
<b>Molecular weight</b>	214.45 g/mole
<b>Color</b>	White
<b>Density</b>	1.45 g/cm <sup>3</sup>
<b>Melting point</b>	80 °C

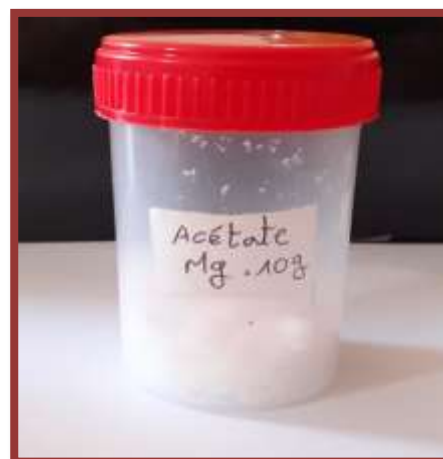


**Figure (II.2) :** magnesium acetate.

## 2.3 The solvent :

The solvent must present a relatively high dielectric constant to dissolve the inorganic salts[3]. Most alcohols are dipolar, amphiprotic solvents with a dielectric constant that is dependent on the chain length [4]. Copper acetate is not miscible in water, Another solvent must be added to the mixture (precursor and catalyst), It is better to use

ethanol (Figure (II.3)), to avoid possible reactions between the various components which modify the kinetics of reactions [5] ,The properties of ethanol are listed in the following table (II.3):

**Table (II-3):** The physical and chemical properties of Ethanol.

<b>Chemical name</b>	Ethanol
<b>Molecular formula</b>	$C_2H_5OH$
<b>Molecular weight</b>	46.07 g/mole
<b>Physical state</b>	Liquid
<b>Density</b>	$0.789 \text{ g/cm}^3$ à $20 \text{ }^\circ\text{C}$
<b>Melting point</b>	$78.37 \text{ }^\circ\text{C}$



**Figure (II.3) :** Ethanol.

## 2.4 Catalyst :

HCL (Figure (II.4)) is very good catalysts for copper acetate, the properties of HCL are listed in the table (II.4):

**Table (II.4):** The physical and chemical properties of HCL.

<b>Chemical name</b>	Hydrochloric acide
<b>Molecular formula</b>	HCL
<b>Molecular weight</b>	36.46 g/mole
<b>Physical state</b>	colorless inorganic chemical system
<b>Density</b>	$1.49 \text{ kg/m}^3$
<b>Melting point</b>	$-114.2 \text{ }^\circ\text{C}$



**Figure (II.4) :**HCL .

### **3 Experimental procedure :**

#### **3.1 Preparation of Substrates :**

##### **3.1.1 Choice of substrates :**

The choice of substrates (Figure (II.5)) is dictated by the physico-chemical properties of the substrates/material pairs to be deposited. We used sheets of glass as a substrates for the following reasons :

- The glass substrates are transparent and insulating, which allows good optical and electrical characterization of our films.
- During the deposition, it is understood that the adhesion of the liquid sol to the substrate is good. This property is ensured by using glass substrates.
- The chemical composition of the glass substrates does not lead to the contamination of our thin films by diffusion of chemical species during annealing.
- For economic reasons (Low cost, Abundance...).
- Low tension between the substrate and the thin films.
- The coefficient of thermal expansion of the substrate can play an important role during the anneals necessary for the densification of the material [6].



**Figure (II.5):** the substrates.

##### **3.1.2 Substrates cut :**

The glass substrates have a dimension of  $(6.5 \times 2.5) \text{ cm}^2$ , its thickness is [1-1.2] mm. They were cut into three equal slides with a dimension of  $(2.4 \times 2.5) \text{ cm}^2$  with a diamond pen (Figure II.6).



**Figure (II.6) : Substrates cut .**

### **3.1.3 Substrats Cleaning Process :**

The quality of sample deposition depends on the cleanliness and surface conditions of the substrate. Cleaning substrates is a very important step that takes place in a clean step because this latter determines the adhesion and homogeneity qualities of the deposited layers. The process used for cleaning glass substrate is described Shown in(Figure II.7) by the following steps:

- Washing with soap solution to clean any dust or attachments.
- Rinsing with distilled water to remove soap.
- The substrates are placed in the Acetone for 10 minute.
- Cleaning in water distilled bath.
- Drying using a drier.

Thus all traces of greases and impurities stuck to the substrate's surface are removed.



**Figure (II.7) : Substrats Cleaning Process.**

### 3.2 Preparation of solutions:

In this work, copper acetate  $[\text{Cu}(\text{CH}_3\text{COO})_2]$  and magnesium acetate  $[\text{Mg}(\text{CH}_3\text{COO})_2]$  was used as the starting materials sources a homogeneous and stable solution with a concentration of 0.2 mol/l. CuO coating solutions were prepared by mixing 0.5898(g) of copper acetate was used as a precursor, Which was weighed using a digital scale (Figure (II.8)), and different doping percentage of magnesium acetate as a source of doping with magnesium (1%.3%.5%.7%.9%) in 15 ml of pure Ethanol ( $\text{C}_2\text{H}_5\text{OH}$ ) was used as a solvent, HCl employed as catalyst it was put into the solution drop by drop like stabilizer to form the precursor solution and the mixture was stirred by a magnetic stirrer (Figure (II.9)) at 60 °C for 2 hours until obtained a clear, transparent and homogeneous solution. Finally, the solution is kept for a while 24 hours at room temperature. Until obtained a clear and slightly viscous and homogeneous solution (Figure (II.10)), which was greenish transparent in nature. Then used for the spin coating step.



**Figure (II.8):** digital scale.



**Figure (II.9):** magnetic stirrer.



**Figure (II.10):** the solution.

### 3.3 Deposition of Thin Films:

#### 3.3.1 Spin coating method:

The deposition procedure comes immediately after the preparation of the substrates and the solution. CuO thin films were elaborated using the Spin Coating process and based on the solutions of copper acetate doped by magnesium acetate previously prepared. The machine which was used to deposit the Mg-doped CuO thin films is described as follows (figure (II.11)) :



**Figure (II.11):** the spin coating machine.

The spin coating method is a simple and cheap method, which provides products of high purity and good homogeneity. In this method, the surfactant, solvents, reaction time, speed and temperature are the main factors that influence the thin film performance .this method is mainly based on the following four steps:

- ❖ Preparation of the precursor solutions.
- ❖ Formation of the sol.
- ❖ Conversion the solution to a gel.
- ❖ Calcination.
- ❖ Deposition.

deposition steps can be recapitulated as follows:

A small amount of 5 ml is taken from the solution using a syringe. it is deposited on the substrate which is mounted on the spin coating machine's support. Then the (substrate-

support) is rotated at a constant speed of rotation. The liquid is thereby spread out along the substrate simultaneously.

### **3.3.2 Heat treatment :**

The deposition step is followed by two other thermal operations essential for the densification of thin films: drying and annealing. They are necessary for obtaining good quality thin films.

### **3.3.3 Drying thin films :**

The drying of the deposited layer is a very important step in the production of quality materials and avoids the creation of cracks in the materials. It corresponds to the evaporation of residual solvents on the substrate surface. Once deposited, the thin films are dried at 200 °C for 10 min in the drying oven (Figure (II.12)). After drying, the films were left in the air for a few minutes before depositing the next film on the previous one. The cycle ( spin/drying) is repeated 6 times to obtain a final film.



**Figure (II.12):** the drying oven.

### 3.3.4 Annealing Thin Films :

This is the last step in the deposition of thin films. After the drying step a dense gel is obtained, this gel undergoes an annealing heat treatment intended for its transformation into a dense film. The density of the layers is obtained after annealing at a fixed temperature of 500°C for 3 hours (figure (II.13)). At the end, the samples are kept at room temperature.



**Figure (II.13):** The annealing furnace.

**Table (II.5):** The parameters used for depositing our thin films.

<b>Solution</b>	<b>Copper acetate + Ethanol + drops HCl + percentage of doping (Mg(CH<sub>3</sub>COO)<sub>2</sub>)</b>					
<b>Morality (mol / l)</b>	<b>0.2</b>					
<b>Solution volume (ml)</b>	<b>15</b>					
<b>Agitation time (h)</b>	<b>2</b>					
<b>Agitation température (° C)</b>	<b>60</b>					
<b>Rotation speed (t/min)</b>	<b>3000</b>					
<b>Deposit time (s)</b>	<b>30</b>					
<b>Drying temperature (° C)</b>	<b>200</b>					
<b>Drying time (min)</b>	<b>10</b>					
<b>Number of repetitions (spin + drying)</b>	<b>6</b>					
<b>Annealing temperature (° C)</b>	<b>500</b>					
<b>Annealing time (h)</b>	<b>3</b>					
<b>Copper acétate mass (g)</b>	<b>0.5989</b>					
<b>Doping percentage (Mg at %)</b>	<b>0</b>	<b>1</b>	<b>3</b>	<b>5</b>	<b>7</b>	<b>9</b>
<b>magnesium acétate mass (g)</b>	<b>/</b>	<b>0.0168</b>	<b>0.0504</b>	<b>0.0840</b>	<b>0.1177</b>	<b>0.1553</b>

The steps for preparing CuO thin film are summarized in the flowchart below :

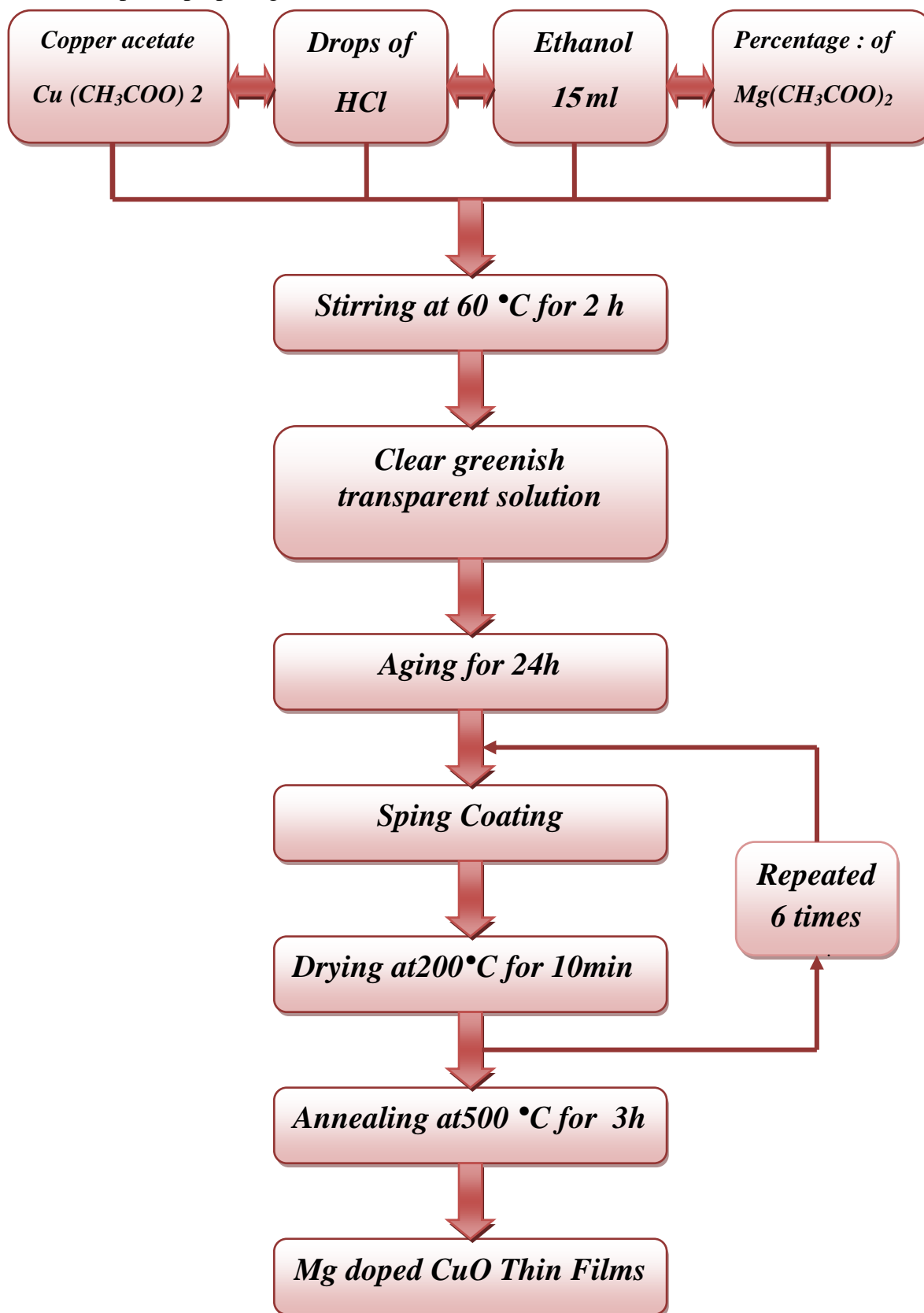


**Figure (II.14):** Flow chart of sol-gel method (spin coating) for preparation of

CuO thin films.

## **4 Characterization Techniques of Thin Films:**

The optimization of the preparation conditions is the main task to get device quality films. The study of CuO requires different characterizations that allow the study of the thin film properties[7]. For these purposes the obtained films have been analyzed by different techniques of characterization:

- ✓ X-ray diffraction (XRD), to study the structural characterization, crystallographic orientation and determination of the size average of the grains and the study of surface qualities.
- ✓ Ultraviolet visible spectroscopy (UV- VIS), for the determination of material thickness, the optical refractive index, optical gap and the disorder.
- ✓ The four-point technique for electrical measurements.

In the following sections, the techniques used for the film characterizations are described briefly.

### **4.1 Structural characterization :**

#### **4.1.1 X-Ray Diffraction (XRD) :**

X-ray diffraction is a widely used method for characterizing the structure of a material. It is a powerful nondestructive technique used in physical, chemical, and biological sciences. It provides information on structures, phases, preferred crystal orientations (texture), and other structural parameters, such as average grain size, crystallinity, strain, and crystal defects. XRD peaks are produced by constructive interference of a monochromatic beam of X-rays scattered at specific angles from each set of lattice planes in a sample. The peak intensities are determined by the atomic positions within the lattice planes. Consequently, the XRD pattern is the fingerprint of periodic atomic arrangements in a given material[8].

##### **4.1.1.1 Principle of analysis:**

The principle of analysis is based on the diffraction of monochromatic X-rays by the atomic planes of the crystals of the material studied in figure (II.14). The incoming beam (coming from upper left) source each scatterer to re-radiate a small portion of its intensity as a spherical wave. So that, there is diffraction. If scatterers are arranged symmetrically with a separation  $d$ , these spherical waves will be in sync (add

constructively) only in directions where their path-length difference  $2d \sin \theta$  equals an integer multiple of the wavelength  $\lambda$ . In that case, part of the incoming beam is deflected by an angle  $2\theta$ , producing a reflection spot in the diffraction pattern. According to **Bragg's** law, then constructive interference occurs equation (II.1) [9] :

$$n\lambda = 2d_{hkl} \sin \theta \quad (\text{II.1})$$

Equation (II.I) Bragg's law describes at which angles and wavelengths an incident x-ray wave will cause constructive interference of the scattered waves.

Where:

- ✓ **n**: is an integer.
- ✓  **$\lambda$** : is the wavelength of the incident wave.
- ✓  **$d_{hkl}$** : is the spacing between the planes in the atomic lattice.
- ✓  **$\theta$** : is the angle between the scattered wave and the atomic plane.

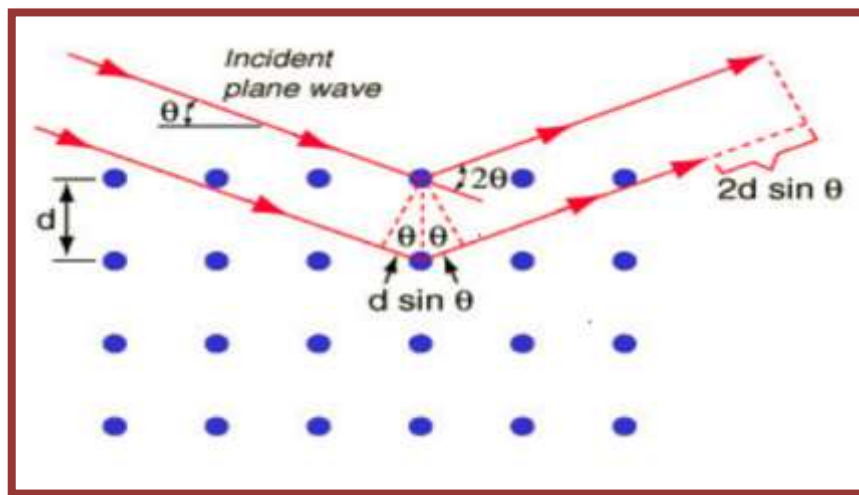


**Figure (II.15):** Diffraction of X-rays by a crystal according to Bragg's law[10].

**4.1.1.2 The apparatus used in this study :**

The structural characterization is carried out by X-ray diffraction in our university. The diffractometer used for the characterization of our samples is of type Bruker D8 Advanced from the Mohammed Khider Biskra University. With  $2\theta = (20^\circ - 80^\circ)$  And the step is  $0.03^\circ$  ,Samples take 20 minutes to characterize. Where it appears the device in Figure (II-16).



**Figure (II.16):** The x-ray diffractometer used in the analysis of x-ray diffraction of the samples.

X-ray Diffractometer consists of three basic elements: an X-ray tube, a sample (maybe powder, single crystal or thin film) holder, and an X-ray detector. (Figure II.17).

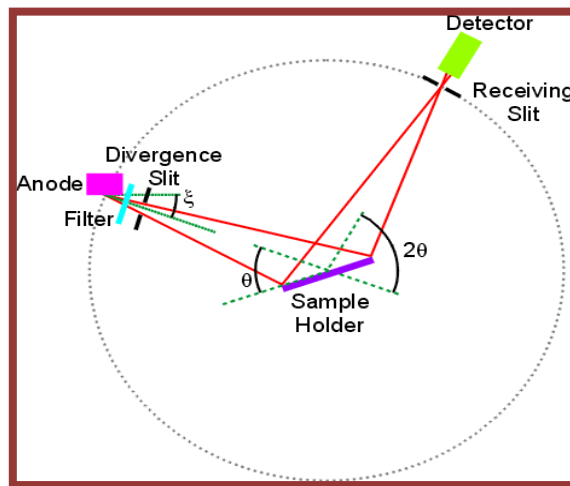


**Figure (II.17):** Diagram of an X-ray Diffractometer[11].

**4.1.1.3 Determination of the inter-reticular distances and the cell parameters:**

The X- ray diffraction data can be used to determine the dimension of the unit cell. The three indices h, k, and l are used to define each plane, which in turn relates to the atomic spacing d. In the simplest form, the relation between d and h, k and l in a monoclinic structure are presented in Equation (II.2) [12]:

$$d_{hkl} = \frac{1}{\sqrt{\frac{h^2}{a^2 \sin^2 \beta} + \frac{k^2}{b^2} + \frac{l^2}{c^2 \sin^2 \beta} - 2 \frac{hl \cos \beta}{ac \sin^2 \beta}}} \quad (\text{II.2})$$

Where:

- ✓ **hkl** : Miller's indices.
- ✓ **a,c** : the cell parameters.
- ✓ **d<sub>hkl</sub>** : inter planer spacing (inter-reticular distance) used in Bragg's law.

And the values of the mesh parameters for different crystallographic systems can be calculated from the following equations using the parameters (**hkl**) and the inter planar spacing (**d**) as shown below [13]:

- Cubic system:  $\frac{1}{d^2} = \frac{h^2+k^2+l^2}{a^2} \quad (\text{II.3})$

**4.1.1.4 Determination of the Grain Size:**

The grain size of the different samples was first determined from the diffraction spectra. To ensure these grain size values, by measuring the width at mid-height (FWHM) of the most intense peaks, then we can estimate the average size (**D**) of the crystallites by **Scherrer's** formula (II.4) which is written below [14]:

$$D = \frac{0.9\lambda}{\beta \cos \theta_{hkl}} \quad (\text{II.4})$$

Where:

- ✓ **θ**: Bragg's angle.
- ✓ **λ**: wavelength of X-ray used.
- ✓ **D**: crystallite size in Å or nm.
- ✓ **β**: full width at half maxima of the peak (FWHM) in radians, as shown in the figure (II.18) below.

The angular width at a point where the intensity has fallen to half of its maximum value (Full width at half maximum intensity or FWHM) is a measure of broadening of x-ray peak [15].

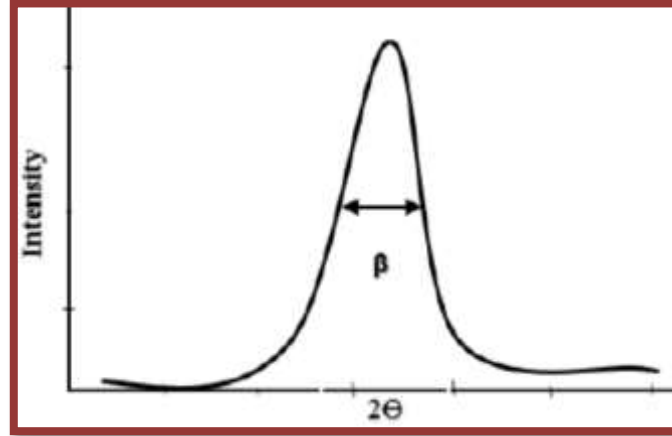


**Figure (II.18):** Determination of  $\beta$ [16].

#### 4.1.1.5 Determination of constraints:

Constraints are internal forces in matter. The relation which connects the constraints ( $\sigma_{ij}$ ), the tensors of strain ( $\epsilon_{kl}$ ) and the constants of elasticity ( $C_{ijkl}$ ) is given by the law of **Hooke** equation (II.5)[17]:

$$\sigma_{ij} = C_{ijkl} \cdot \epsilon_{kl} \quad (\text{II.5})$$

For the calculation of these constraints, it is necessary to have the values of the elastic constants, The constants of elasticity are not always available in the literature (as in the case of our material), and as long as the deformation varies in a proportional way with the stress, one can use this relationship between its two variables to get an idea about the variation of the stresses of the layers studied and this with the help of the formula of the following deformation (II.6)[18]:

$$\epsilon = \frac{\beta \cos \theta}{4} \quad (\text{II.6})$$

Where:

- ✓  $\theta$ : is the Bragg's angle.
- ✓  $\beta$ : is the full width at half maximum (FWHM) of the peak.

**4.1.1.6 Determination of Dislocations' density:**

Knowing the grain size values (**D**), we can estimate the density of the dislocation (**δ**), which is defined as the length of the dislocation lines per unit of the crystal's volume, using the formula of **Williamson** and **Smallman**, Shown by the equation (II.7) [19]:

$$\delta = \frac{1}{D^2} \quad \text{(II.7)}$$

**4.2 Optical characterization:**

**4.2.1 Ultraviolet-visible spectroscopy (UV- VIS) :**

UV-Visible spectroscopy is the measurement of the intensity of absorption of nearultraviolet and visible light by a sample. Ultraviolet and visible light are energetic enough to promote outer electrons in an atom to higher energy levels. UV-Vis spectroscopy is usually applied to molecules and inorganic ions or complexes in solution or solid samples. The UV- Vis spectra have broad features that are of limited use for sample identification but it is a very useful technique for quantitative measurements. Moreover, UV-Vis spectroscopy is used to determine the optical band gap transitions of semiconductors [20] . The absorption or reflectance in the visible range directly affects the perceived colour of the chemicals involved. In this region of the electromagnetic spectrum, molecules undergo electronic transitions. This technique is complementary fluorescence spectroscopy, in that fluorescence deals with transitions from the excited state to the ground state, while absorption measures transitions from the ground state to the excited state [21].

**a) The principle of this technique:**

This technique based on the knowledge of the distances between interference rings in the spectra of transmission in the visible and the near-infrared. One uses a recording spectrophotometer with double beams [22], the ratio between the intensity of the beam transmitted by a sample **I** and the initial intensity **I<sub>0</sub>** is called transmittance **T** and is usually expressed as a percentage (%**T**) or absorbance **A** Which is expressed by the equation (II.8), spectrophotometer principle of operation is represented, as shown in the figure (II.19) [23].

$$A = -\log\left(\frac{T}{100}\%\right) \quad \text{(II.8)}$$

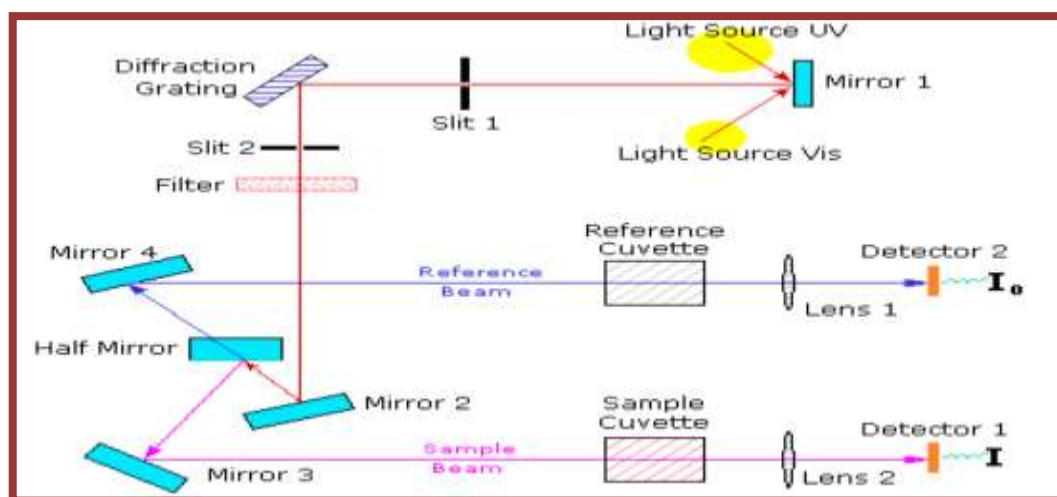


**Figure (II.19):** The principle of operation of UV-visible [24].

**b) The apparatus used in this study:**

The transmission spectrometer used is Perkin Elmer LAMBDA 25 UV/ VIS Spectrometer (Figure (II.20)) with double beam one for their reference (glass) the other with the sample (glass – film). their spectral range extends from wavelength  $\lambda=200$  nm to 800 nm. Spectra obtained gives the variation of transmittance expressed as a percentage according to their wavelength.



**Figure (II.20):** ultraviolet-visible spectrophotometer (LAMBDA 25).

Besides, using the interferences, one can determine the following parameters: The Thickness of the film, the absorption coefficient, the optical gap, the disorder, in addition to the refraction index which can be calculated using the following relations:

**4.2.2 The Thickness of the Film:**

There are several ways to measure the thickness of thin films, including:

**4.2.2.1 The Approximate Gravimetric Method :**

The thickness of the thin films can be calculated using the approximate gravimetric method.

the substrate is weighed before and after deposition using a very sensible balance. Knowing the density of the material (thin film) and the surface of the substrate, the thin film thickness can be determined using the following relationship (II.9) [25]:

$$t = \frac{\Delta m}{P_t \times A_0} \tag{II.9}$$

Where:

- ✓  $P_t$ : the density of the film.
- ✓  $A_0$ : the surface of the substrate.
- ✓  $t$ : the thickness of the thin film.

**4.2.2.2 Measurement of thickness by interference fringe method:**

By the way, thanks to the interference, we can determine the thickness of the thin films of CuO. The physical constants used in the calculations are defined in the figure (II.21):

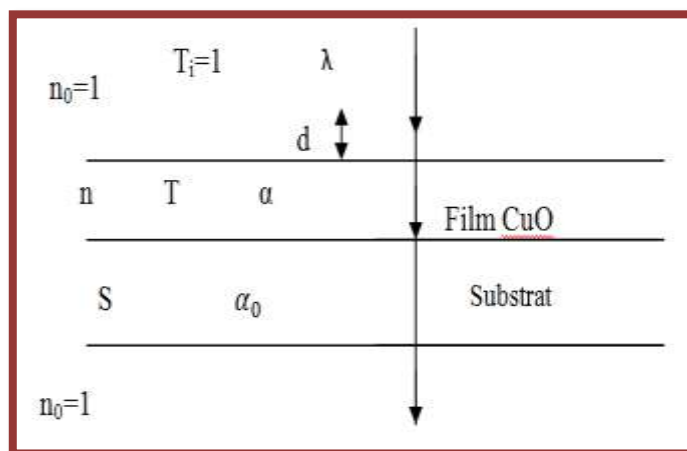


**Figure (II.21):** The physical constants used in the calculations.

Where  $T$  is the transmittance,  $\alpha$  is the absorption coefficient of the film,  $\lambda$  is the incidental light wavelength,  $n$  and  $s$  are the refraction indexes of the film and the substrate respectively and  $d$  represents the film thickness. Using the physical parameters defined in figure (II.22) and the spectrum of transmission obtained, one can determine the film thickness, by using equation (II.10):

$$d = \frac{\lambda_1 \lambda_2}{2(\lambda_2 n_1 - \lambda_1 n_2)} \quad \text{(II.10)}$$

Where:  $n_1$  and  $n_2$  are the refraction index of the film for the wavelength  $\lambda_1$  and  $\lambda_2$  respectively; we can

calculate  $n_1$  and  $n_2$  from the following relation (II.11):

$$n_{1,2} = [N_{1,2} + (N_{1,2}^2 + S^2)^{\frac{1}{2}}]^{\frac{1}{2}} \quad \text{(II.11)}$$

And  $N_{1,2}$  can be obtained using this relation (II.12):

$$N_{1,2} = \frac{2S(T_M - T_{m1,2})}{T_M T_{m1,2}} + \frac{S^2 + 1}{2} \quad \text{(II.12)}$$

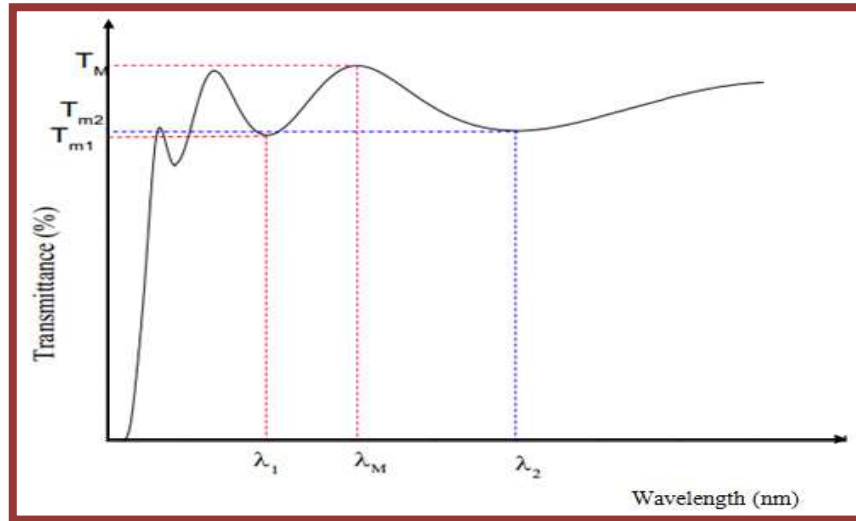


**Figure (II.22):** Method of interference fringes to determine the thickness[26].

#### 4.2.3 Determination of the absorption coefficient:

In the spectral field where the light is absorbed, and by knowing the film's thickness, we can determine the absorption coefficient for each value of transmittance  $T$  (%) using Beer-Lambert's law (II.13):

$$T = \frac{I}{I_0} \times 100 \quad (\text{II.13})$$

Where:

$$\frac{I}{I_0} = \exp(-\alpha d) = \frac{T}{100} \quad (\text{II.14})$$

Where:

- ✓ **d**: the thickness of the film.
- ✓  **$\alpha$** : coefficient of absorption.
- ✓ **I**: the transmitted light intensity.
- ✓  **$I_0$** : is the incidental light intensity.

✚ This relation can be written as:

$$\alpha = \frac{1}{d} \ln\left(\frac{I_0}{I}\right) \quad (\text{II.15})$$

If we express T ( $\lambda$ ) in (%), this expression becomes:

$$\alpha = \frac{1}{d} \ln\left(\frac{100}{T}\right) \quad (\text{II.16})$$

This approximate relation is established, by neglecting the reflections on all interfaces; (air/film, air/substrate)[27].

#### **4.2.4 Determination of the optical gap:**

There are several ways to determine the optical gap Among them :

- ❖ Method of the second derivative of the absorption function :

The method of the second derivative is to determine the value of the optical gap by drawing the second optical absorption derivative as a function of the Photon Energy, and the maximum absorbed energy corresponding to the first transition representing the optical range is determined by using the minimum value of the curve representing the second derivative :

$$Eg = \frac{hc}{\lambda_{min}} = \frac{12400}{\lambda_{min}} \quad (\text{II.17})$$

Where:

- ✓ **Eg** is the optical gap.

- ✓ **h** is Planck's constant.
- ✓ **C** is Speed of light in vacuum.
- ❖ Absorption coefficient method (Model Tauc):

In this method, the determination of the visual gap depends on the model proposed by Tauc, The absorption coefficient is related to the optical band gap via Tauc's equation [22]:

$$(\alpha h\nu)^n = A(h\nu - E_g) \quad \text{(II.18)}$$

Where:

- ✓ **E<sub>g</sub>** is the optical gap.
- ✓ **n** and **A**: are constants.
- ✓ **hν** is the photon energy.
- 🌈 **n** characterizes the optical type of transition and takes the values (1/2, 2), (**n=1/2** for allowed direct transitions or **n=2** for allowed indirect transitions)[19].

To determine the nature of the transition in the films produced in this study, we will plot the curves  $(\alpha h\nu)^2 = f(h\nu)$ .

By extending the linear part from  $(\alpha h\nu)^2$  to the abscissa axis ( $(\alpha h\nu)^2 = 0$ ) we can obtain **E<sub>g</sub>** value as it showing in figure (II.23) [28]:

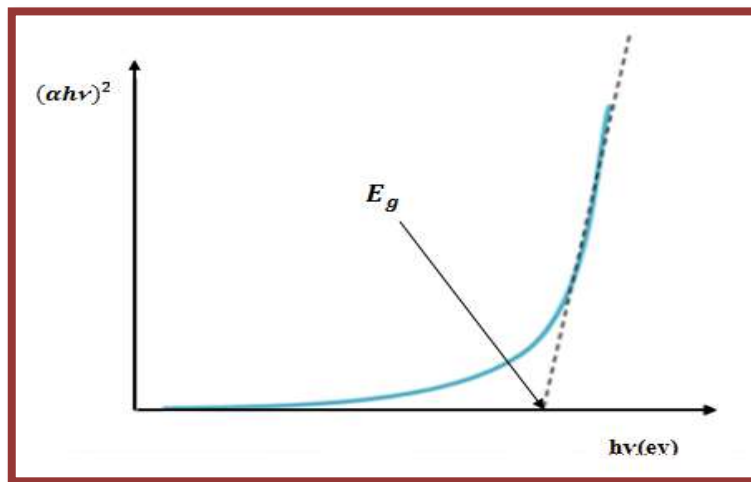


**Figure (II.23):** Determining the energy gap  $E_g$  [19].

#### 4.2.5 Determination of The disorder (the energy of Urbach):

The empirical parameter  $E_{00}$  often referred to the Urbach tails, has the dimensions of energy and is frequently used to determine the film quality (measures the degree of

disorder in amorphous semiconductors)[29], In this work, the Urbach tail is used as a parameter for assessing the amount of disorder in doped CuO films. According to Urbach's law, the expression of the absorption coefficient is written as follows [30]:

$$\alpha = \alpha_0 \exp\left(\frac{hv}{E_{00}}\right) \quad (\text{II.18})$$

Where:

- ✓  $\alpha_0$ : is constant.
- ✓  $E_{00}$ : urban energy.

By drawing the  $\ln(\alpha)$  as a function of  $hv$ , one can determinate  $E_{00}$  value:

$$\ln(\alpha) = \ln(\alpha_0) + \frac{hv}{E_{00}} \quad (\text{II.19})$$

The following figure presents how we can estimate  $E_{00}$  [27].

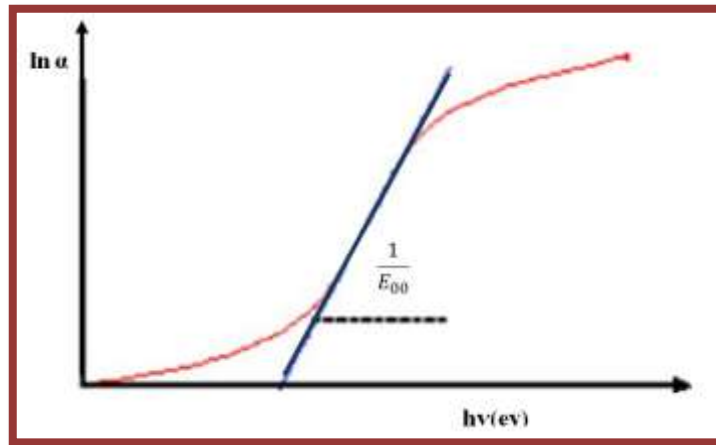


**Figure (II.24):** Determination of the disorder by extrapolation from the variation of  $\ln(\alpha)$  as a function of  $hv$ [27].

#### 4.2.6 Determination of the refractive index:

The refractive index is reduced when the gap energy increases according to the following relation[31]:

$$n^2 = 1 + \left(\frac{A}{E_g + B}\right) \quad (\text{II.20})$$

Where:

- ✓ **A** and **B** are constant; **A=13.6 eV** , **B=3.4 eV** .
- ✓ **E<sub>g</sub>**: the experimental value of the energy band.



# *Bibliography*

[1]: Ch. Saadia, « L'effet de dopage par l'aluminium sur les propriétés des couches minces de TiO<sub>2</sub> élaborées par voie Sol-Gel (spin coating) », Mémoire De Master, Université Mohamed Khider – Biskra ,2017.

[2]: Z. fatma , « Elaboration et caractérisation des couches minces d'oxyde de Titane (TiO<sub>2</sub>) à différentes nombres des couches par voie Sol-Gel (spin coating) », Mémoire De Master, Université Mohamed Khider – Biskra ,2018.

[3]: Y. Natsume, H. Sakata, «Thin Solid Films»,vol 372, pp.30–36,2000.

[4]: L. Armelao, M. Fabrizio, S. Gialanella, F. Zordan, «Thin Solid Films»,vol 394, pp.90–96,2001.

[5]: A.Taklit , « Dopage et caractérisation des couches minces d'oxyde de Titane( TiO<sub>2</sub>) élaborées par voie sol-gel: L'effet du taux de chlorure d'Aluminium », Mémoire De Master ,Université Mohamed Khider – Biskra ,2018.

[6]: K. Younes, « Elaborations et caractérisations des couches minces d'oxyde de titane par voie sol gel : effet de la vitesse de rotation » , Mémoire De Master, Université Mohamed Khider – Biskra ,2016.

[7]: A.Olzick, « Deposition, characterization, and fabrication of Zinc Oxide Piezoelectric thin film micro speaker using dc reactive sputtering », Master Thesis ,University of San Luis Obispo, 2012.

[8]:F.Sima, C.Ristoscu, L.Duta ,O.Gallet, K.Anselme, I.N.Mihailescu, « Laser Surface Modification of Biomaterials», Techniques and Applications, Journal of science direct ,Pages 77-125,2016.

[9]: B. E. Warren, « X-Ray Diffraction»,Books, Kindle Edition, 2012.

[10] :[Http://Serc.Carleton.Edu/Research\\_Education/Geochemsheets/Techniques/Xrd.Html](http://Serc.Carleton.Edu/Research_Education/Geochemsheets/Techniques/Xrd.Html).

[11] : <https://images.app.goo.gl/9KHeYLGLjJYSPbUq6>.

[12] : P. Gravereau, « Introduction à la pratique de la diffraction des rayons X par les poudres », université de Bordeaux, 2012.

[13]: A. Aldrin, «Preparation and characterization of certain II-VI, I-III-VI<sub>2</sub> semiconductor thin films and transparent conducting oxides », PhD thesis, Cochin University of Science and Technology, Kerala, India, 2004.

[14] : S. Benramache , «Elaboration Et Caractérisation Des Couches Minces De Zno Dopées Cobalt Et Indium », Thèse De Doctotrat Université Mohamed Khider – Biskra ,2012.

[15]: X. Wang, P. Clark, and S. T. Oyama, «Synthesis, characterization, and hydrotreating activity of several iron group transition metal phosphides », Journal of Catalysis, vol. 208, pp. 321-331, 2002.

[16]: C. Khelifi, A. Attaf, H. Saidi, A. Yahia, M. Dahnoun, and A. Saadi, «Effect of solution flow on the properties of tin dioxide SnO<sub>2</sub> thin films deposited by spray pyrolysis technique », Optik-International Journal for Light and Electron Optics, vol. 127, pp. 11055-11062, 2016.

[17] : A. Mourad, «Elaboration et caractérisation des couches minces d'oxyde de silicium, obtenues par voie sol-gel », Mémoire de magister, université de Constantine ,2010.

[18] : H. Barkahoum, «Etude des propriétés optiques des nanocristaux du semi-conducteur CdS dispersés dans des films minces du polymère polystyrène et de la silice SiO<sub>2</sub>», Mémoire de Magister, Université Mentouri Constantine ,2006.

[19] : I. bouhaf kherkhachi, « Study of Thin layers of Tin Sulfide (SnS) Elaborated by Chemical Means for technological applications», thèse de doctorat, Université Med Khider – Biskra,2016.

[20]: A. Hauser, «Intersystem crossing in Fe (II) coordination compounds», Coordination Chemistry Reviews, vol. 111, pp. 275-290, 1991.

[21]: S. Ratiba, «The Effect of Annealing Temperature On The Characteristics of NiO:Co Thin Films», Mémoire de Master, Université Med Khider – Biskra,2016.

[22]: M. Boubeche, « Molarity Effect on the Properties of Indium Oxide Thin Films Deposited By Ultrasonic Spray Technique», Master dissertation, Mohamed Khider University, Biskra, Algeria, 2011.

[23]: H. Sheikh, « Separation of copper-oxide nanoparticles from nanoparticle enhanced phase change material », thèse de Master, University of Alabama, 2013.

[24]: <https://images.app.goo.gl/WMaiyxxUYZDRpkwR7>.

[25]: S. Abdel Hakim, «Rotational speed and solvent effect on the structural and optical properties of zno thin films prepared by sol-gel (spin coating) metho», Mémoire de Master, Université Med Khider – Biskra,2014.

[26]: H. Benelmadjat, «Elaboration Et Caractérisation Des Composites Dopés Par Des Agrégats Nanométriques De Semi-Conducteurs», Thèse de Magister, université de Constantine , 2007 .

[27]: M. Boubeche, «Molarity Effect on the Properties of Indium Oxide Thin Films Deposited by Ultrasonic Spray Technique», Master dissertation, Mohamed Khider University, Biskra, Algeria, 2011.

[28]: A. Taabouche, « Etude structurale et optique de films minces ZnO élaborés par voie physique et/ou chimique », thèse de doctorat, Université Frères Mentouri–Constantine, 2015.

[29] : J. A. Olley, «Solid State Communications», vol 13 (9), pp. 1437-1440, 1973.

[30]: D. Redfield, Physical Review, vol 130 (3), pp. 914-918, 1963.

[31]: A. bouderdabene, «Elaboration et caractérisation des couches minces de NiO dopé par le chrome (Cr)», Mémoire de Master, Université Med Khider – Biskra,2017.

**Chapter III:**

***Results and Discussion .***

## 1 Introduction:

This chapter includes the description and the analysis of the measurements and the discussion of the results. It focuses on the optical properties of copper oxide CuO thin films doped by different percentages of Mg (1%.3%.5%.7%.9%).

## 2 Optical Properties of Mg Doped CuO Thin Films :

The optical measurements were carried out using Perkin Elmer LAMBDA 950 UV/ VIS spectrophotometer. Wave length spectral ranges between 200 nm and 800 nm.

In what follows, we present and discuss the results related to optical gap, Urbach's energy, absorption coefficient, reflection R, the extinction coefficient K, the refractive index n, absorbance and the Transmittance spectra of the films.

### 2.1 Transmittance spectra:

The optical transmittance spectra of cuo films doped by different percentages of Mg are shown in figure (III.1).

According to the results, all the transmittance values of the films are between 25% and 75%; noticing that unlike the other films, 1% and 3% films record the less value of transmittance in the visible range, while 9% records the highest one (75%).

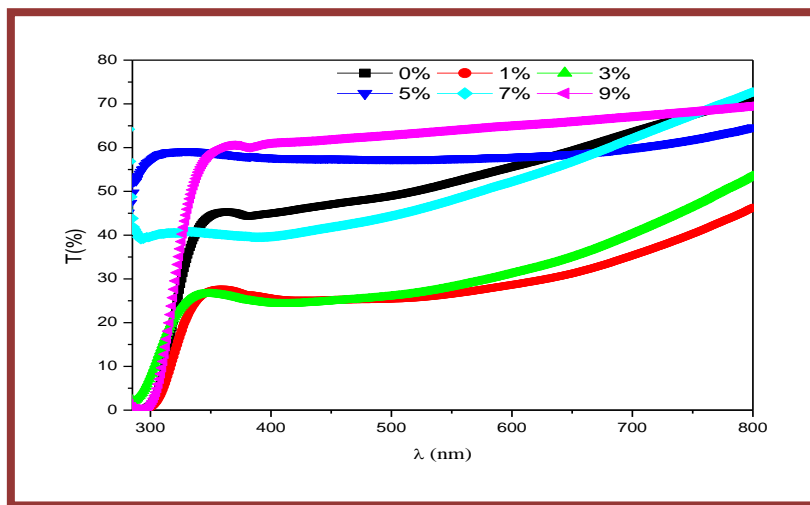


**Figure (III.1):** Optical transmittance spectra of Mg CuO thin films as a function of wavelength.

## 2.2 Absorbance spectra:

Figure (III.2) displays the absorbance spectra of the different Mg doped CuO thin films. It is clear that 1% and 3% absorb more than 50% of the incident photons, and the other films have less absorbance values than 50%, almost less than 30% for 9%. This latter can be considered as transparent film in this range of waves.

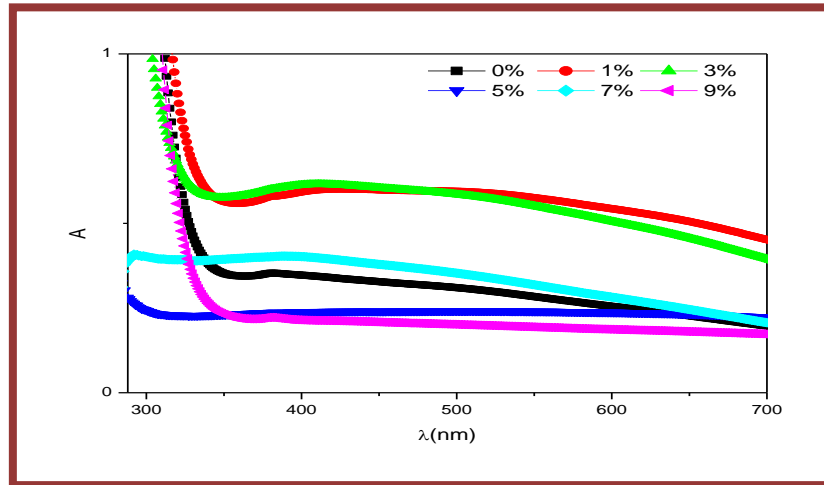


**Figure (III.2):** Optical absorbance spectra of Mg CuO thin films as a function of wavelength.

## 2.3 The absorption coefficient:

The absorption coefficient is given by the following relationship [1]:

$$\alpha = 2.303 \frac{A}{d} \quad (\text{III.1})$$

Where:

- ✓ A: is the absorbance of the films.
- ✓ d: is the thickness of the films.

d is determined using HebalOptics program. The average thickness is found equal 237, 83 nm. The coefficient absorption of the CuO thin films doped by different percentages of Mg as function of wave length is illustrated in the figure (III.3).

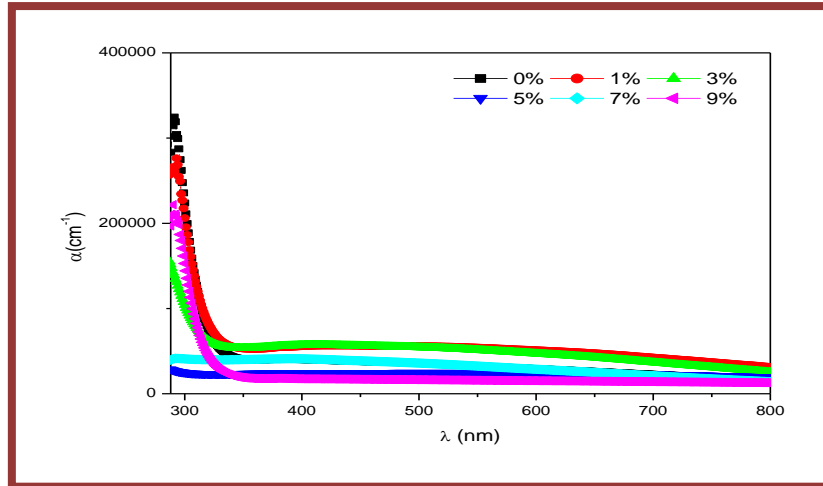


**Figure (III.3):** The absorption coefficient of Mg doped CuO as a function of the wavelength.

$\alpha$  curves show an exponential decrease with increasing length wave giving rise to two absorption areas; up to 340 nm almost all the Mg doped CuO films absorb a great amount of incident photons which is characterized by a high value of  $\alpha$ , beyond 340 nm all the films are characterized by a low value of absorption coefficient, thus; photons are poorly absorbed and the films appear transparent to that wavelength.

## 2.4 The optical Gap ( $E_g$ ) :

The optical gap  $E_g$  is related to the absorption coefficient  $\alpha$  by the following relationship:

$$\alpha h\nu = A(h\nu - E_g)^m \quad (\text{III.2})$$

The optical gap of CuO was found, direct optical band gap so  $m = \frac{1}{2}$  [2], and it evaluated by extrapolating the straight line part of the curves  $(\alpha h\nu)^2$  with energy axes  $(h\nu)$  i.e.  $(\alpha h\nu)^2 = 0$ . Figure (III.4) shows the dependence of  $(\alpha h\nu)^2$  to the energy  $(h\nu)$  for as-deposited and doped CuO films.

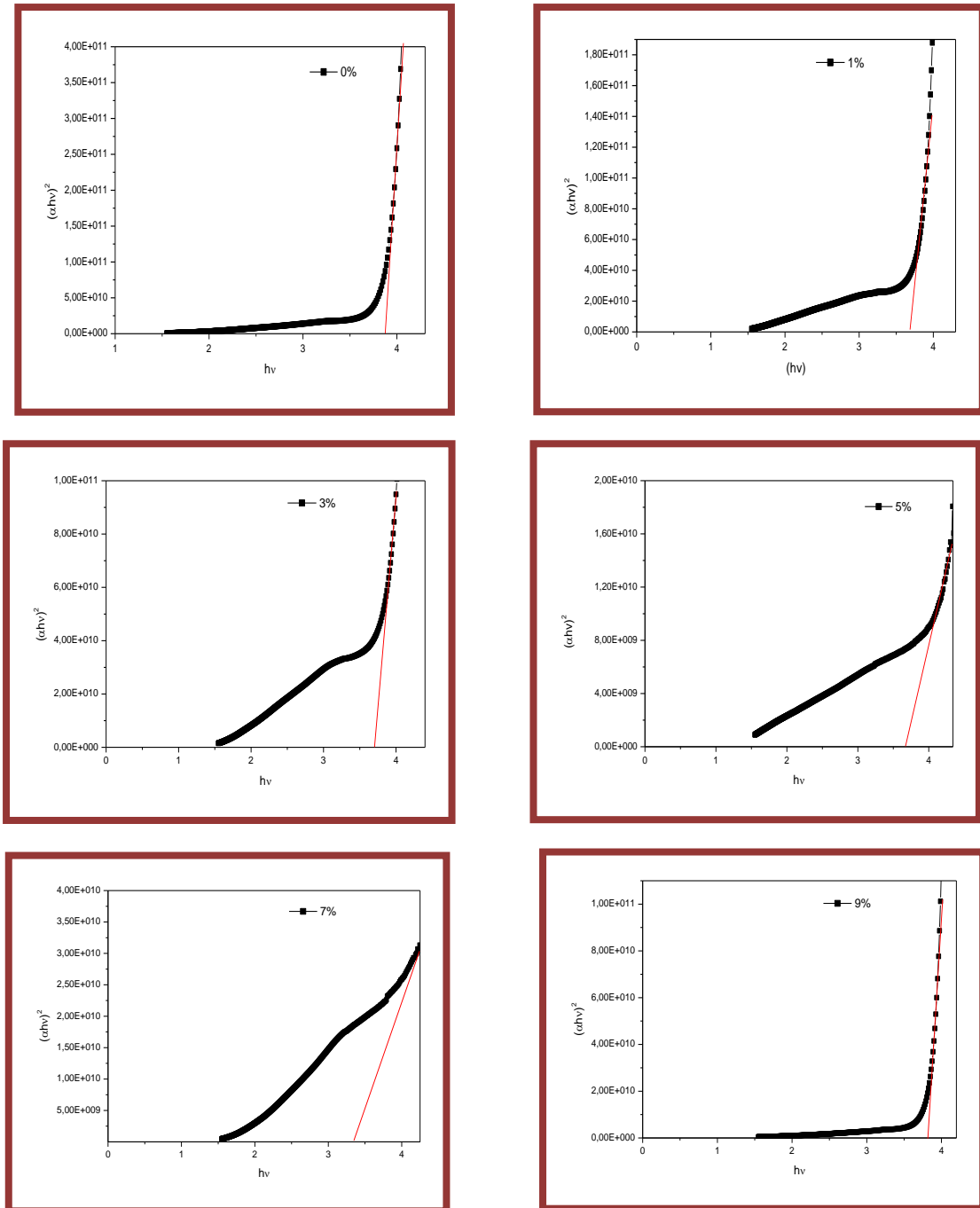


**Figure (III.4):** The variation of  $(\alpha hv)^2$  as a function of  $hv$  for each Doping percentage.

The values of  $E_g$  determined from figure (III.4) are listed in table (III.1) and depicted in Figure (III.5). It is found that the obtained values of  $E_g$  decrease with the increasing of the percentage of the Mg doping except for the case of 9%. The result of this latter could be excluded due to its unusual behavior. This behavior could be

related to the Fermi level of Mg doping which gives rise to band tails in the band gap of CuO which in turn leads to the effective decrease in the band gap.

**Table (III.1):** Optical gap values.

Doping percentage (Mg at %)	0	1	3	5	7	9
E <sub>g</sub> (eV)	3.879	3.722	3.703	3.668	3.372	3.803

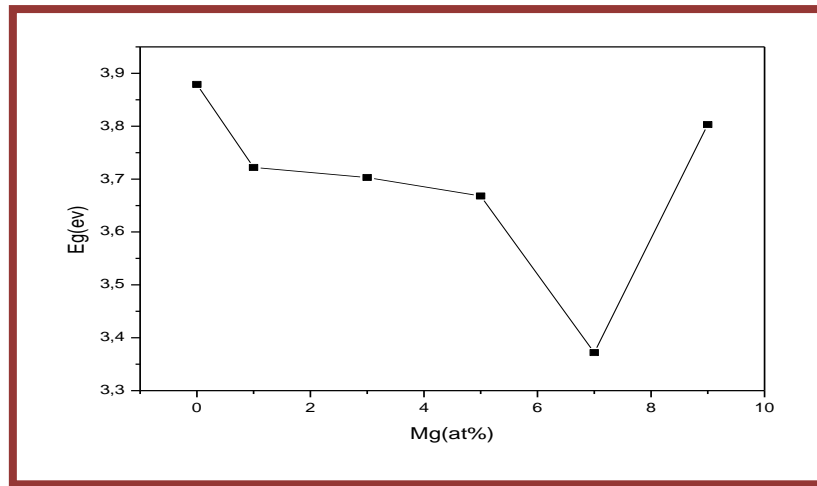
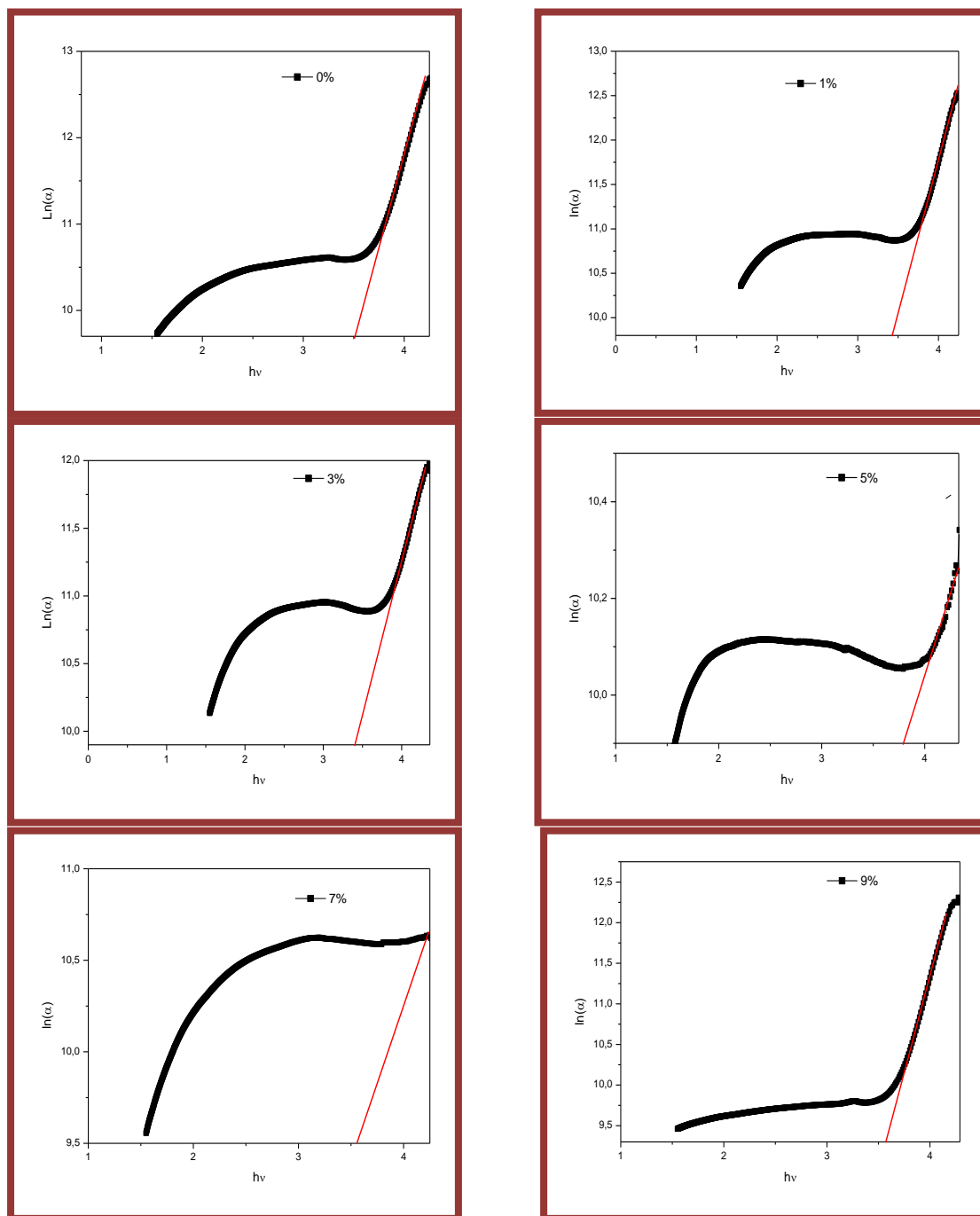


**Figure (III.5):** Effect of doping ratio on the gap band E<sub>g</sub>.

## 2.5 The Disorder (Urbach energy):

The same thing as the optical gap, using the method indicated in the paragraph (2.4) we can draw the curves for each doping percentage (figure III.6). The obtained values of the Urbach energy are displayed in table (III.2) and illustrated in figure (III.7).

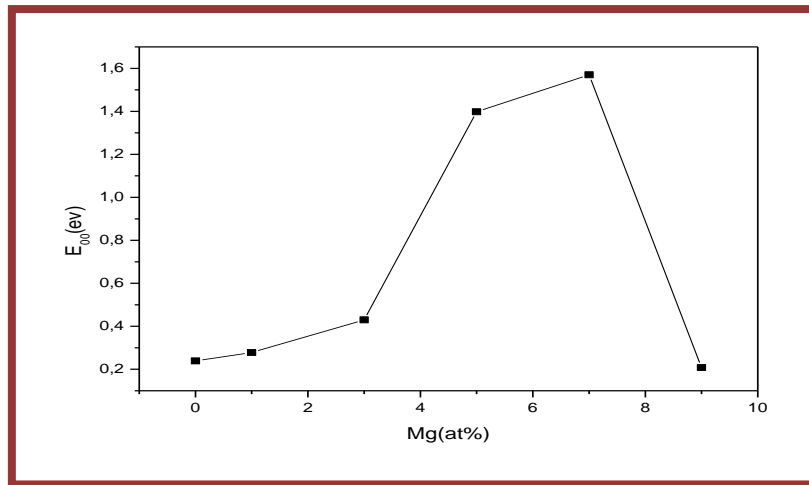
As we can see from this figure, the disorder energy increases as the ratio of the Mg doping increases except for the case of 9% which could be excluded for the same reason said before. The behavior of the disorder energy with respect to the doping ratio could be justified by the fact that increasing doping gives rise to localized states or defects which decrease the band gap and increase the disorder in the host material.



**Figure (III.6):** Variations of  $\ln(\alpha)$  as a function of  $h\nu$ .

**Table (III.2):** Disorder's (Urbach energy) values.

Doping percentage (Mg at %)	0	1	3	5	7	9
Urbach energy: $E_{00}$ (eV)	0.239	0.278	0.430	1.398	1.570	0.208

**Figure (III.7):** effect of doping ratio on the disorder energy  $E_{00}$ .

## 2.6 The reflection:

Reflection spectrum is calculated from absorption and transmission spectrum according to the following equation [3]:

$$\mathbf{T + A + R = 1 \quad \rightarrow \quad \mathbf{R = 1 - T - A} \quad \text{(III.3)}$$

Figure (III.8) illustrate reflection spectrum of CuO films for different doping ratio. Increased doping ratio doesn't lead to an increase in the reflection values maybe this due to the different thicknesses of the elaborated films because it is difficult to control the film thickness using spin coating method.

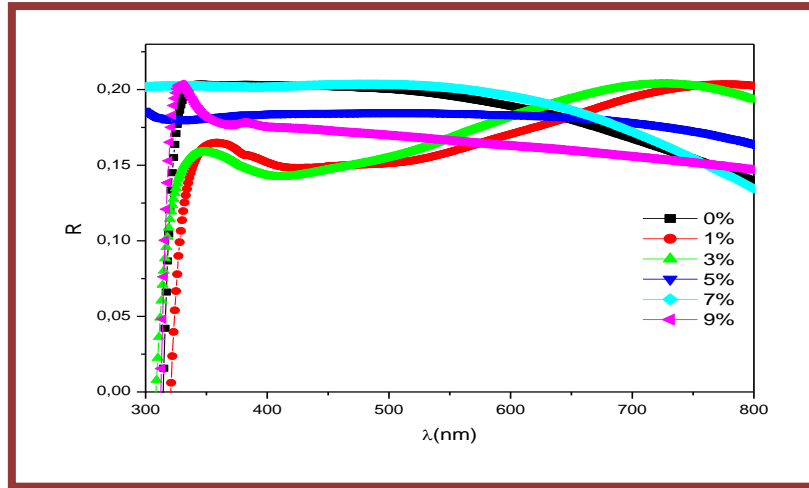


**Figure (III.8):** Optical reflection spectrum of Mg doped CuO films as a function of wavelength.

## 2.7 The extinction coefficient K:

The extinction coefficient  $k$  characterizes the attenuation of the incident light energy as it passes through the material; this coefficient is proportional to the optical absorption as shown in the following relation [4]:

$$k = \frac{\lambda}{4\pi} \alpha(\lambda) \quad (\text{III.4})$$

The extinction curves of the Mg doped CuO thin films as a function of wavelength are depicted in Figure (III.9). The extinction coefficient depends on absorbance, so that the behavior of all curves is similar to absorption spectra. It's clear that the extinction coefficient of our films ranges between (0.05 and 0.27).

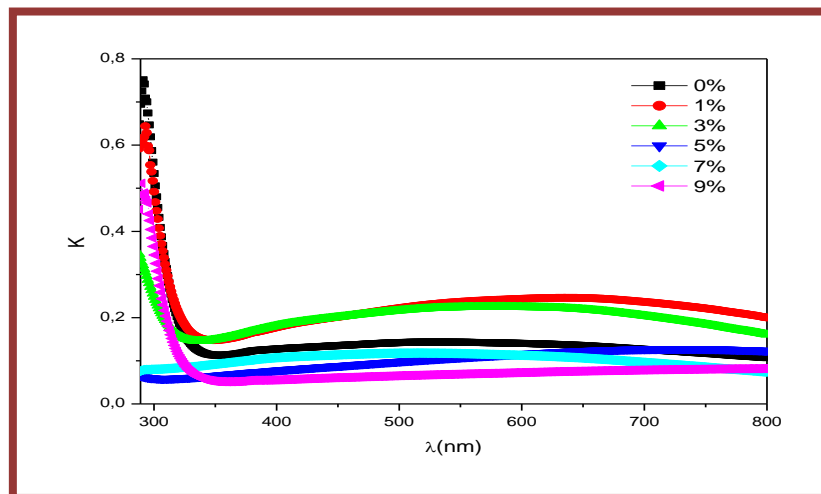


**Figure (III. 9):** Variation of the extinction index as a function of the wavelength.

## 2.8 The refractive index $n$ :

The refractive index characterizes the attenuation of the propagation speed of the light wave as it passes through the material. The refractive index is defined by [5]:

$$n = \left[ \left( \frac{1+R}{1-R} \right)^2 - (k^2 + 1) \right]^{1/2} + \frac{1+R}{1-R} \quad (\text{III.5})$$

Figure (III.10) shows the behavior of refractive index for Mg doped CuO films. The result shows that the refractive index of our samples varies in the visible range between 2.2 and 2.6.

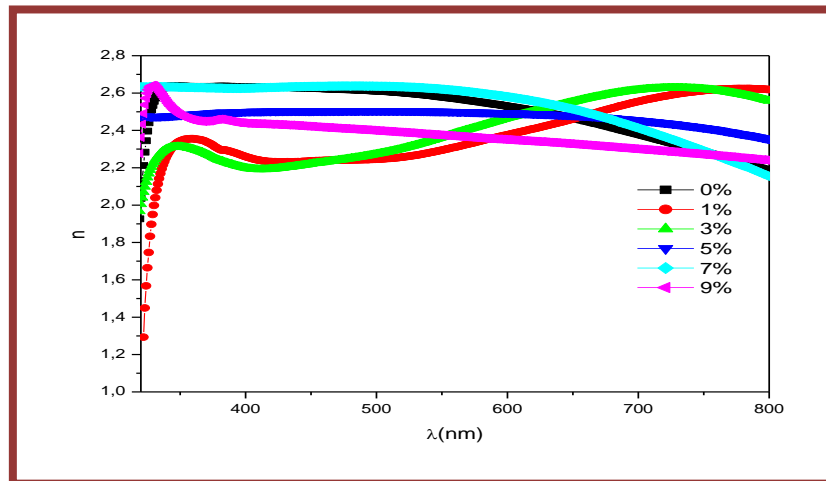


**Figure (III.10):** the refractive index profile of Mg doped CuO films.



# *Bibliography*

[1]:K.N.Manjunatha, S.Paul, *Applied Surface Science*, 352 (2015) 10-15.

[2]:M. Boubeche, « Molarity Effect on the Properties of Indium Oxide Thin Films Deposited by Ultrasonic Spray Technique», Master dissertation, Mohamed Khider University, Biskra, Algeria, 2011.

[3]: K. L. Chopra, « Thin Film Phenomena », Mc. Graw-Hill, New York, (1985).

[4]: H. U. Lgwe, O. E. Ekpe and E. I. Ugwu, *J. Applied science , Engineering and technology*, vol. 2, P. 447, (2010).

[5]: S. O. Kasap, «Principles of Electronic Materials and Devices», 2nd ed., McGraw-Hill, New York, (2002).



*General Conclusion*

## *General Conclusion.*

---

### **General Conclusion:**

During this work, we were interested in the deposition and characterization of Mg doped CuO thin films, elaborated by the Sol-Gel spin-coating technique on glass substrates.

The goal of the work is to study the influence of doping percentage on the properties of the prepared this films namely optical properties. Thus, 0.5898 g of copper acetate was used as a precursor, as source of doping, we used magnesium with different ratios (1%.3%.5%.7%.9%).

The optical characterization in the range of 200 nm to 800 nm, our films are absorbent in the UV region. However in visible region, the films 1% and 3% have an absorption more than 50% and those of 0%, 5% ,7% and 9% have an absorbance less than 50% and . Regarding the optical transmittance spectra of the CuO films with different ratios of Mg, results showed that the transmittance ranges between (25% to 75%). they show also that the obtained values of  $E_g$  decreases with the increasing of the percentage of Mg doping, except for 9%.

It is found that the disorder energy increases with the increase in almost all Mg doping.

The extinction coefficient depends on the absorbance. The extinction factor for our films ranges between 0, 05 and 0, 27, while reflection values ranges between (0.15 to 0.25) and the refractive index of the elaborated films are between (2.2 to 2.6).

Finally, we conclude from all the experimental results of our study that doping percentages affect the optical properties of CuO thin films.

## توليف وتوصيف أفلام رقيقة من أكسيد النحاس المطعم بالمغنيزيوم.

### ملخص:

في هذا العمل التطبيقي قمنا بترسيب شرائح رقيقة لأكسيد النحاس CuO النقية و المطعمه بالمغنيزيوم Mg, بنسب مختلفة من التطعيم (0%-1%-3%-5%-7%-9%) على مساند زجاجية باستعمال تقنية سائل- هلام) طريقة الترسيب باللف). مع تثبيت باقي الوسائط كتركيز المحلول, سرعة الدوران, وقت التلدين و حرارة التلدين. الشرائح تم تحضيرها انطلاقا من محاليل أسيتات النحاس المذابة في خليط من الإيثانول, و أسيتات المغنيزيوم كمصدر للمطعم. الهدف من هذا العمل هو دراسة إمكانية تحسين الخصائص البصرية لرقائق أكسيد النحاس العينات تم توصيفها باستعمال مطيافية الأشعة فوق البنفسجية والمرئية. تظهر النتائج التجريبية أن: الأفلام 1% و 3% ,تسجل أقل قيمة للنفاذية في النطاق المرئي, بينما تسجل 9% أعلى قيمة (75%). أما بالنسبة لأطياف الامتصاص من الواضح ان 1% و 3% تمتص أكثر من 50% من الفوتونات الساقطة, النطاق البصري وجد أنه يتناقص مع زيادة نسبة المطعم على العموم تتراوح قيمته ما بين (3.372 ev إلى 3.879 ev), اما بالنسبة الانعكاسية فتتراوح بين (0.15 إلى 0.25) و قرينة انكسار الافلام ما بين (2.2 إلى 2.6).

الكلمات المفتاحية: الشرائح الرقيقة, المغنيزيوم المطعم, أكسيد النحاس, الخصائص البصرية.

## **Synthesis and Characterization of Mg Doped CuO Thin films.**

### **Abstract:**

In this study we deposited non doped and Mg doped CuO thin films with different doping ratios (0%-1%-3%-5%-7%-9%) onto glass substrates by sol gel spin coating method with setting other parameters such as the concentration of the solution, rotational speed, the annealing time and annealing temperature, The prepared films were obtained by dissolving copper acetate in a mixture of ethanol and magnesium acetate as doped source. Our main goal is the study of the possibility to enhance the optical properties of CuO thin films. To achieve our goal, Mg doped thin films were analyzed by the UV-Visible spectroscopy. The experimental results show that: all the transmittance values of the films are between 25% and 75%, 1% and 3% films record the less value of transmittance in the visible range, while 9% records the highest one (75%). As for the absorption spectra, 1% and 3% absorbs more than 50 % of the incident photons; it was found that the optical gap decreases with the increasing doping percentage, its value ranges between (3.372 ev to 3.879 ev). Whereas, the Reflection of the films is between 0.15 and 0.25, and the refractive index varies between (2.2 to 2.6).

**Key words:** Thin films, Magnesium dopant, CuO, Optical properties.

## **Synthèse et caractérisation des couches minces de CuO dopées par Mg.**

### **Résumé :**

Dans ce travail nous avons déposé des couches minces CuO non dopées et dopées par Mg avec différents pourcentages de dopage (0% -1% -3% -5% -7% -9%) sur des substrats du verre par la méthode sol gel (sping-coating) en maintenant les autres paramètres fixe tel que la concentration de la solution, la vitesse de rotation, la durée et la température de recuit. Les couches minces ont été obtenues à partir des solutions de l'acétate de cuivre dissous dans un mélange de l'éthanol et l'acétate de magnésium comme source de dopant. Le but de ce travail est d'étudier la possibilité d'améliorer les propriétés optiques des couches minces de CuO. Les échantillons ont été analysés par la spectroscopie UV-Visible (UV-Vis). Les résultats expérimentaux ont montré que: toutes les valeurs de la transmittance des couches sont comprises entre 25% et 75%, notant que les films 1% et 3% enregistrent la moindre valeur de transmittance dans le domaine visible, tandis que 9% enregistre la valeur la plus élevée (75%). Quant aux spectres d'absorption, les films de 1% et 3% absorbent plus de 50% des photons incidents, il a été trouvé que globalement le gap optique diminue avec l'augmentation du pourcentage de dopage Sa valeur varie entre (3.372 ev de 3.879 ev), quant à la réflexion, elle varie entre (0.15 de 0.25) et la valeur de l'indice de réfraction des films est comprise entre (2.2 de 2.6).

**Mots clés:** Couches minces, Magnésium dopé, CuO, propriétés optiques.

بِسْمِ اللَّهِ الرَّحْمَنِ الرَّحِيمِ